


Efficient proximity labeling in living cells and organisms with TurboID

Tess C Branon^{1–4}, Justin A Bosch⁵, Ariana D Sanchez⁴, Namrata D Udeshi⁶ , Tanya Svinkina⁶, Steven A Carr⁶, Jessica L Feldman⁴, Norbert Perrimon^{5,7} & Alice Y Ting^{1–4,8}

Protein interaction networks and protein compartmentalization underlie all signaling and regulatory processes in cells. Enzyme-catalyzed proximity labeling (PL) has emerged as a new approach to study the spatial and interaction characteristics of proteins in living cells. However, current PL methods require over 18 h of labeling time or utilize chemicals with limited cell permeability or high toxicity. We used yeast display-based directed evolution to engineer two promiscuous mutants of biotin ligase, TurboID and miniTurbo, which catalyze PL with much greater efficiency than BioID or BioID2, and enable 10-min PL in cells with non-toxic and easily deliverable biotin. Furthermore, TurboID extends biotin-based PL to flies and worms.

Enzyme-catalyzed PL is an alternative to immunoprecipitation and biochemical fractionation for proteomic analysis of macromolecular complexes, organelles, and protein interaction networks¹. In PL, a promiscuous labeling enzyme is targeted by genetic fusion to a specific protein or subcellular compartment. Addition of a small-molecule substrate, such as biotin, initiates covalent tagging of endogenous proteins within a few nanometers of the promiscuous enzyme (**Fig. 1a**). Subsequently, the biotinylated proteins are harvested using streptavidin-coated beads, and identified by mass spectrometry (MS).

Two enzymes are commonly used for PL: APEX2, an engineered soybean ascorbate peroxidase^{2,3}; and BioID, a promiscuous mutant of *Escherichia coli* biotin ligase^{4,5}. The advantages of APEX2 are its speed—proximal proteins can be tagged in 1 min or less^{6,7}—and its versatility, as APEX2 also captures endogenous RNAs⁸ and generates contrast for electron microscopy⁹. However, APEX labeling requires the use of H₂O₂, which is toxic to living samples. By contrast, BioID labeling is simple and non-toxic: only biotin needs to be supplied to initiate tagging. This feature has resulted in >100 applications of BioID since its introduction 5 years ago, in cultured mammalian cells^{5,10,11}, plant protoplasts¹², parasites^{13–21}, slime mold^{22,23}, mouse²⁴, and yeast²⁵.

The major disadvantage of BioID, however, is its slow kinetics, which necessitates labeling with biotin for 18–24 h (and sometimes much longer²⁴) to produce sufficient biotinylated material

for proteomic analysis. This precludes the use of BioID for studying dynamic processes that occur on the timescale of minutes or even a few hours. Furthermore, the low catalytic activity makes BioID difficult or impossible to apply in some contexts, such as in worms, flies, or the endoplasmic reticulum lumen of cultured mammalian cells. Recently, new promiscuous biotin ligase variants, BioID2 (ref. 26) and BASU²⁷, have been reported, but the former still requires >16 h of labeling^{26,28–30}, while BASU enriched a proteome of only two proteins²⁷. Further characterization (see below) shows that the activities of BioID, BioID2, and BASU are all comparable.

A new PL enzyme that combines the simplicity and non-toxicity of BioID with the catalytic efficiency of APEX2 would greatly enhance PL applications. To achieve this, we undertook the directed evolution of *E. coli* biotin ligase (BirA) to generate new promiscuous mutants. To begin, we compared BioID (BirA-R118G) to seven other mutations at the R118 position. We found that R118S is about twofold more active than R118G under identical conditions (**Supplementary Figs. 1 and 2** for all full blot images and **Supplementary Note 1**), and hence we selected this mutant rather than BioID as our starting template for evolution.

As in previous work^{3,31}, we combined yeast surface display of our enzyme library with fluorescence-activated cell sorting (FACS) to perform the evolution. We used error-prone PCR to mutagenize BirA-R118S, generating a library of ~10⁷ mutants, each with an average of about two amino acid mutations relative to template. This library was then displayed on the yeast surface as a fusion to the Aga2p mating protein (**Fig. 1b**). We added biotin and ATP to the yeast pool to initiate promiscuous biotinylation, followed by streptavidin-fluorophore to stain biotinylation sites on the surface of each yeast cell. FACS was used to enrich cells displaying a high degree of self-biotinylation over cells displaying low or moderate self-biotinylation (**Fig. 1b**). We gradually reduced the biotinylation time window from 18 h to 10 min over 29 rounds of selection, in order to progressively increase selection stringency (**Supplementary Note 1** and **Supplementary Fig. 3**).

We encountered some technical hurdles during the evolution. First, the activity of our starting template (R118S) and input library were too low to be detected on the yeast surface. Thus, we used tyramide signal amplification (TSA³²) on the yeast surface to boost the biotin signal

¹Department of Chemistry, Massachusetts Institute of Technology, Cambridge, Massachusetts, USA. ²Departments of Genetics, Stanford University, Stanford, California, USA. ³Department of Chemistry, Stanford University, Stanford, California, USA. ⁴Department of Biology, Stanford University, Stanford, California, USA. ⁵Department of Genetics, Harvard Medical School, Boston, Massachusetts, USA. ⁶Broad Institute of MIT and Harvard, Cambridge, Massachusetts, USA. ⁷Howard Hughes Medical Institute, Boston, Massachusetts, USA. ⁸Chan Zuckerberg Biohub, San Francisco, California, USA. Correspondence should be addressed to A.Y.T. (ayting@stanford.edu).

Received 23 September 2017; accepted 2 July 2018; published online 20 August 2018; doi:10.1038/nbt.4201

(Fig. 1c and Supplementary Fig. 3b) until the activity of the pool was high enough to no longer require it. Second, to avoid enriching mutants that strongly tagged their own lysine residues but failed to biotinylate neighboring proteins, we treated yeast with the reducing agent TCEP in some rounds of selection, to cleave off the ligase after the biotinylation reaction (Supplementary Fig. 3c). Finally, we introduced negative selection to deplete mutants that exhibited strong biotinylation activity before exogenous biotin addition, because the ability to utilize the low levels of biotin naturally present in yeast media would result in loss of user control of the labeling window (Supplementary Fig. 3f).

Our engineering efforts yielded two promiscuous ligases: 35 kD TurboID, with 15 mutations relative to wild-type BirA; and 28 kD miniTurbo, with the N-terminal domain deleted and 13 mutations relative to wild-type BirA (Fig. 1d, Supplementary Table 1 and Supplementary Note 2). Fig. 1e and Supplementary Fig. 4 show the activity of these ligases on the yeast surface in a side by side comparison to BioID, BirA-R118S, and various intermediate clones from our evolution (G1-G3Δ).

To test TurboID and miniTurbo in mammalian cells, we expressed them in the cytosol of HEK 293T cells. Labeling was initiated with the addition of 50 or 500 μM (C_T) exogenous biotin and terminated by cooling cells to 4 °C and washing away excess biotin (Supplementary Fig. 5). Streptavidin blot analysis of whole cell lysates showed that TurboID and miniTurbo biotinylated endogenous proteins much more rapidly than BioID, giving ~3- to 6-fold difference in signal at early time points, and ~15- to 23-fold difference in signal at later time points (Fig. 1f,g, Fig. 2a,b, Supplementary Fig. 4b, and Supplementary Fig. 6).

We included the newer promiscuous ligases BioID2 (ref. 26) and BASU²⁷ in the comparison, and after normalization to account for differences in ligase expression levels, their activities were similar to that of BioID (Fig. 2a,b). Notably, TurboID gave nearly as much biotinylated product in 10 min as BioID/BioID2/BASU gave in 18 h (Fig. 2a,b). Overall, miniTurbo was 1.5- to twofold less active than TurboID, but exhibited less labeling before addition of exogenous biotin; this feature makes miniTurbo potentially superior for precise temporal control of the labeling window. The resulting trends were

the same when we ran the same experiment with 50 μM biotin instead of 500 μM biotin for labeling (Supplementary Fig. 6c–e).

To compare ligases by a different modality, we also fixed ligase-expressing HEK 293T cells after biotinylation, stained them with neutravidin-fluorophore, and performed confocal microscopy. TurboID and miniTurbo gave clearly detectable biotinylation in most transfected cells after 10 min of biotin labeling (Supplementary Fig. 7). By contrast, BioID, BioID2, and BASU-catalyzed biotinylation was undetectable even at 1 h, and only dimly detectable at 6 h in a small fraction of transfected cells.

Different organelles have distinct pH, redox environments, and endogenous nucleophile concentrations, which may influence PL activity. We therefore compared TurboID, miniTurbo, and BioID in the nucleus, mitochondrial matrix, ER lumen, and ER membrane of HEK 293T cells (Fig. 2c). We found that the absolute activities of each ligase, as well as the relative activities between ligases, varied across compartments (Supplementary Note 3). However, TurboID signal was clearly detectable after 10 min in each compartment, and even stronger than BioID 18-h labeling in the mitochondrial matrix and ER lumen. TurboID was superior to miniTurbo in each of these four organelles. Given our observations, we recommend that users test both TurboID and miniTurbo for PL applications, given the context-dependent variations in their activities.

We next evaluated TurboID and miniTurbo in full-scale proteomic experiments. We asked whether 10-min labeling with these ligases would produce proteomic data sets of similar quality to BioID labeling for 18 h, in terms of specificity, coverage, and labeling radius (Supplementary Note 4 and Supplementary Fig. 8). We selected three mammalian organelles for the analysis: the mitochondrial matrix, nucleus, and ER membrane (ERM)-facing cytosol (Fig. 2d–h and Supplementary Figs. 9–11). Because the ERM is continuous with the cytosol, it is valuable for assessing labeling radius; a good PL enzyme should strongly enrich ERM-localized proteins over immediately adjacent cytosolic proteins.

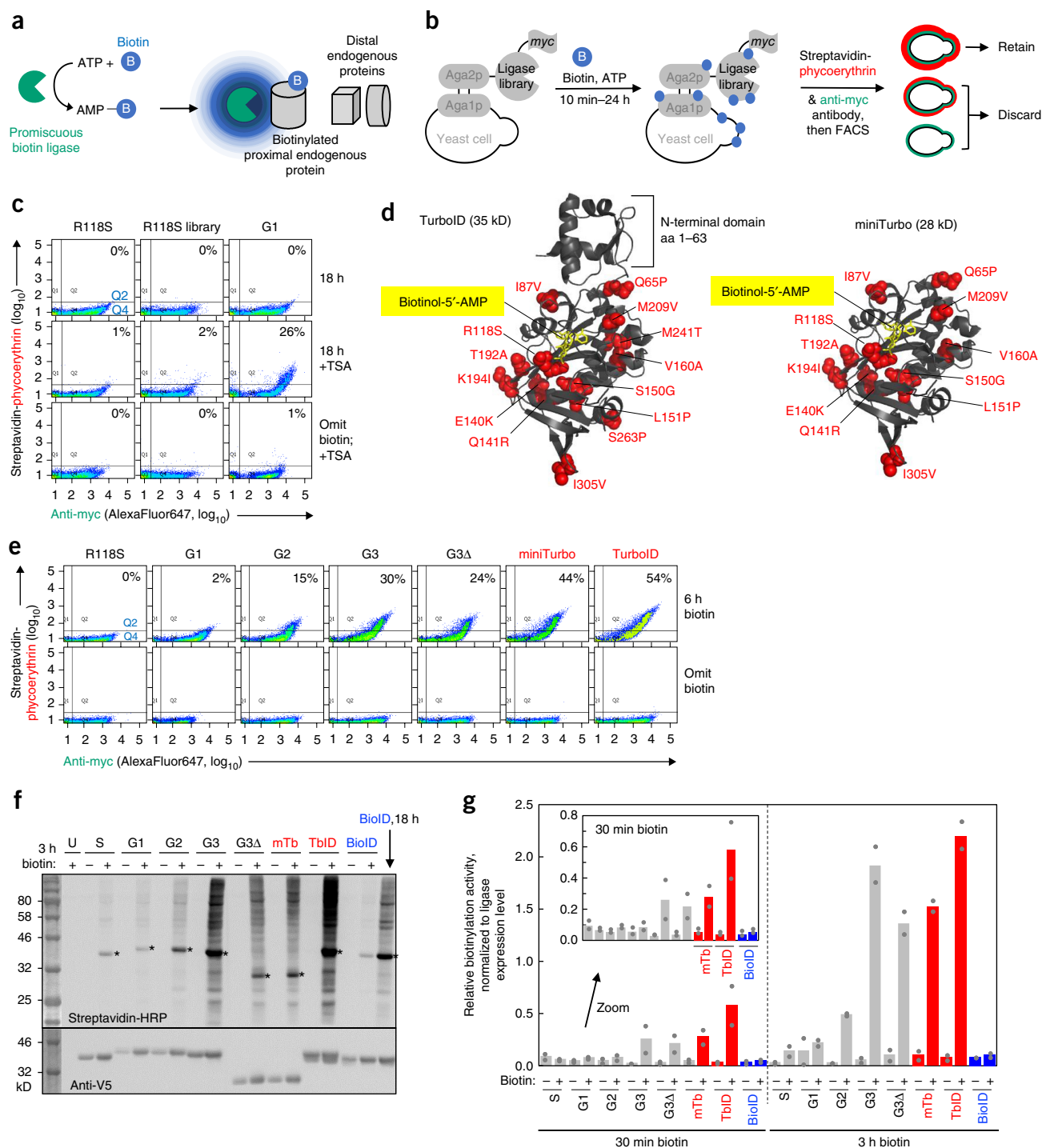
The HEK293T samples we prepared for proteomic analysis are depicted in Figure 2d and Supplementary Figure 10a. TurboID and miniTurbo labeling were each performed for 10 min, whereas BioID

Figure 1 Directed evolution of TurboID. (a) Proximity-dependent biotinylation catalyzed by promiscuous biotin ligases. Ligases catalyze the formation of biotin-5'-AMP anhydride, which diffuses out of the active site to biotinylate proximal endogenous proteins on nucleophilic residues such as lysine. (b) Yeast-display-based selection scheme. A $>10^7$ library of ligase variants is displayed on the yeast surface as a fusion to mating protein Aga2p. All ligases have a C-terminal myc epitope tag. Biotin and ATP are added to the yeast library for between 10 min and 24 h. Ligase-catalyzed promiscuous biotinylation is detected by staining with streptavidin-phycoerythrin and ligase expression is detected by staining with anti-myc antibody. Two-dimensional FACS sorting enables enrichment of cells displaying a high ratio of streptavidin to myc staining. (c) tyramide signal amplification (TSA)³² improves biotin detection sensitivity on the yeast surface. In the top row, the three indicated yeast samples (G1 is the winning ligase mutant from the first generation of evolution) were labeled with exogenous biotin for 18 h then stained for FACS as in b. The y-axis shows biotinylation extent, and the x-axis quantifies ligase expression level. In the second row, after 18 h of biotin incubation, yeast were stained with streptavidin-HRP, reacted with biotin-phenol^{2,32} to create additional biotinylation sites (TSA protocol), then stained with streptavidin-phycoerythrin and anti-myc antibody before FACS. The third row omits biotin. Percentage of cells in upper right quadrant (Q2/(Q2+Q4)) shown in top right of each graph. This experiment was performed once, but each yeast sample was analyzed under identical conditions at least twice in separate experiments with similar results. (d) *E. coli* biotin ligase structure (PDB: 2EWN) with sites mutated in TurboID (left) and miniTurbo (right) shown in red. The N-terminal domain (aa1–63) is also removed from miniTurbo. A non-hydrolyzable analog of biotin-5'-AMP, biotinol-5'-AMP, is highlighted in yellow. (e) FACS plots summarizing progress of directed evolution. G1-G3 are the winning clones from generations 1–3 of directed evolution. G3Δ has its N-terminal domain (aa1–63) deleted. 'Omit biotin' samples were grown in biotin-deficient media for the entire induction period (~18–24 h). This experiment was performed twice with similar results, except G3Δ 'omit biotin', which was performed once. All results shown here were performed side by side in a single experiment. (f) Comparison of ligase variants in the HEK cytosol showing that TurboID and miniTurbo are much more active than BioID, as well as the starting template BirA-R118S and various intermediate clones from the evolution. Indicated ligases were expressed as NES (nuclear export signal) fusions in the HEK cytosol. 50 μM exogenous biotin was added for 3 h, then whole cell lysates were analyzed by streptavidin blotting. Ligase expression detected by anti-V5 blotting. U, untransfected. S, BirA-R118S. Asterisks indicate ligase self-biotinylation. BioID labeling for 18 h (50 μM biotin) shown for comparison in the last lane. This experiment was performed twice with similar results. All results shown here were performed side by side in a single experiment. (g) Quantitation of streptavidin blot data in f and from a 30-min labeling experiment shown in Supplementary Figure 4b. Quantitation excludes self-biotinylation band. Sum intensity of each lane is divided by the sum intensity of the ligase expression band; ratios are normalized to that of BioID/18 h, which is set to 1.0. Gray dots indicate quantitation of signal intensity from each replicate, colored bars indicate mean signal intensity calculated from the two replicates.

labeling was carried out for 18 h. Cells were lysed and biotinylated proteins enriched with streptavidin beads. After on-bead digestion of proteins to peptides, we chemically labeled the peptides with isotopically distinct TMT (tandem mass tag) labels. This enabled us to quantify the relative abundance of each protein across samples. After liquid chromatography (LC)-MS/MS analysis of pooled peptides, we filtered the data via receiver operating characteristic (ROC) analysis (**Supplementary Fig. 9c** and **Supplementary Fig. 10f,g**), using true-positive and false-positive protein lists for each organelle (**Supplementary Tables 2–4**)^{2,33}, to obtain BioID-, TurboID-, and

miniTurbo-derived proteomes for the ERM (**Supplementary Table 5**), nucleus (**Supplementary Table 6**), and mitochondrial matrix (**Supplementary Table 7**).

TurboID- and miniTurbo-derived 10-min proteomes had similar size and specificity as BioID-derived 18-h proteomes in all three compartments (**Figure 2e–h**). In particular, we note that TurboID was just as effective as BioID in enriching secretory proteins over cytosolic proteins when localized to the ERM (**Fig. 2e–g**), suggesting a similar labeling radius despite much faster labeling kinetics. Depth of coverage was similar in the mitochondrial matrix and ERM for the three



ligases, but slightly lower for TurboID and miniTurbo in the nucleus (Supplementary Figs. 9f and 10j).

Given the extremely high activity of TurboID, we wondered whether increasing the labeling time would produce a bigger and better proteome. For the ERM, we found that 1-h labeling with TurboID did increase proteome size by 46% compared to 10-min labeling, but at the expense of specificity (Fig. 2e). With increased labeling time, proximal nucleophiles may become saturated with biotin, enabling TurboID-generated biotin-AMP to travel farther and biotinylate distal, non-specific proteins.

Despite the widespread application of BioID, there have been only two *in vivo* demonstrations to date^{24,34}, which may be related to BioID's low catalytic activity. We wondered whether TurboID and miniTurbo's increased activity might enable biotin-based PL in new settings. We first tested these ligases in bacteria (*E. coli*) and yeast (*Saccharomyces cerevisiae*). As in mammalian cells, TurboID and miniTurbo were considerably more active than BioID (Fig. 3a,b). In particular, we and others²⁵ observe that BioID activity was nearly undetectable in yeast, perhaps in part because yeast is cultured at 30 °C whereas BioID functions optimally at 37 °C²⁶. Because we carried out our directed evolution in yeast at 30 °C, TurboID and miniTurbo exhibit high activity at 30 °C.

BioID has not previously been reported in flies (*Drosophila melanogaster*) or worms (*Caenorhabditis elegans*), despite their appeal as highly genetically tractable model organisms. To test biotin-based PL in flies, we expressed BioID, TurboID, or miniTurbo selectively in the larval wing disc, which gives rise to the adult wing, and raised animals on biotin-containing food for 5 d from early embryo stages (Fig. 3c). TurboID- and miniTurbo-catalyzed biotinylation were 22-fold and ten-fold higher, respectively, than BioID-catalyzed biotinylation, as shown by staining of dissected wing discs with streptavidin-fluorophore (Fig. 3d,e). Consistent with our observations in HEK 293T cells, TurboID also gives some low biotinylation signal in flies fed regular, non-biotin supplemented, food.

We also generated flies expressing BioID, TurboID, or miniTurbo in all tissues (*Act-Gal4* driver, Fig. 3f,g), in muscle (*Mef2-Gal4* driver,

Supplementary Fig. 12a,b), and in all tissues at non-permissive temperature (*tub-Gal4/tub-Gal80^{ts}* driver, Supplementary Fig. 12c,d). Animals were raised on either biotin-containing food from early-embryo stages to adulthood (13 d) (Fig. 3f,g), or regular food to adulthood (13 d), and then switched to biotin-supplemented food for 4 or 16 h (Supplementary Fig. 12). Streptavidin blotting of whole fly lysate showed extensive biotinylation in TurboID and miniTurbo flies, as early as 4 h post-biotin addition (Supplementary Fig. 12), but no signal was detectable in BioID flies, even after 13 d of biotin exposure (Fig. 3g). The absence of detectable BioID signal here, compared to the wing experiment (Fig. 3d), may have resulted from endogenous biotinylated proteins drowning out specific signal in the streptavidin blot.

To test for possible toxicity of TurboID, miniTurbo, and BioID expression in flies, we performed morphological and survival assays. We observed no evidence of toxicity when any of the ligases were expressed tissue-specifically. However, we did find a decrease in fly viability and size when TurboID was expressed ubiquitously and constitutively, and exogenous biotin was withheld (Supplementary Fig. 13, Supplementary Note 5, and Supplementary Fig. 14). Under these conditions, TurboID may consume all the biotin, effectively starving cells of biotin.

We also tested BioID, TurboID, and miniTurbo in *C. elegans*. We expressed the ligases early in the intestinal lineage (~150 min after the first cleavage) and assessed biotinylation activity ~4 h later, at the embryonic bean stage (stage 1), ~5.5 h later at the embryonic comma stage (stage 2), or 3 d later in the adult worm (Fig. 3h). TurboID and miniTurbo were significantly more active than BioID by both imaging and streptavidin blotting at all observed developmental stages (Fig. 3i,j and Supplementary Fig. 15). We also observed that TurboID was expressed at higher levels than miniTurbo expression in adult worms, resulting in much stronger labeling (Fig. 3i and Supplementary Fig. 15g). TurboID and miniTurbo labeling yield could be further increased by raising worms at higher temperatures (25 °C vs. 20 °C; Supplementary Fig. 15g).

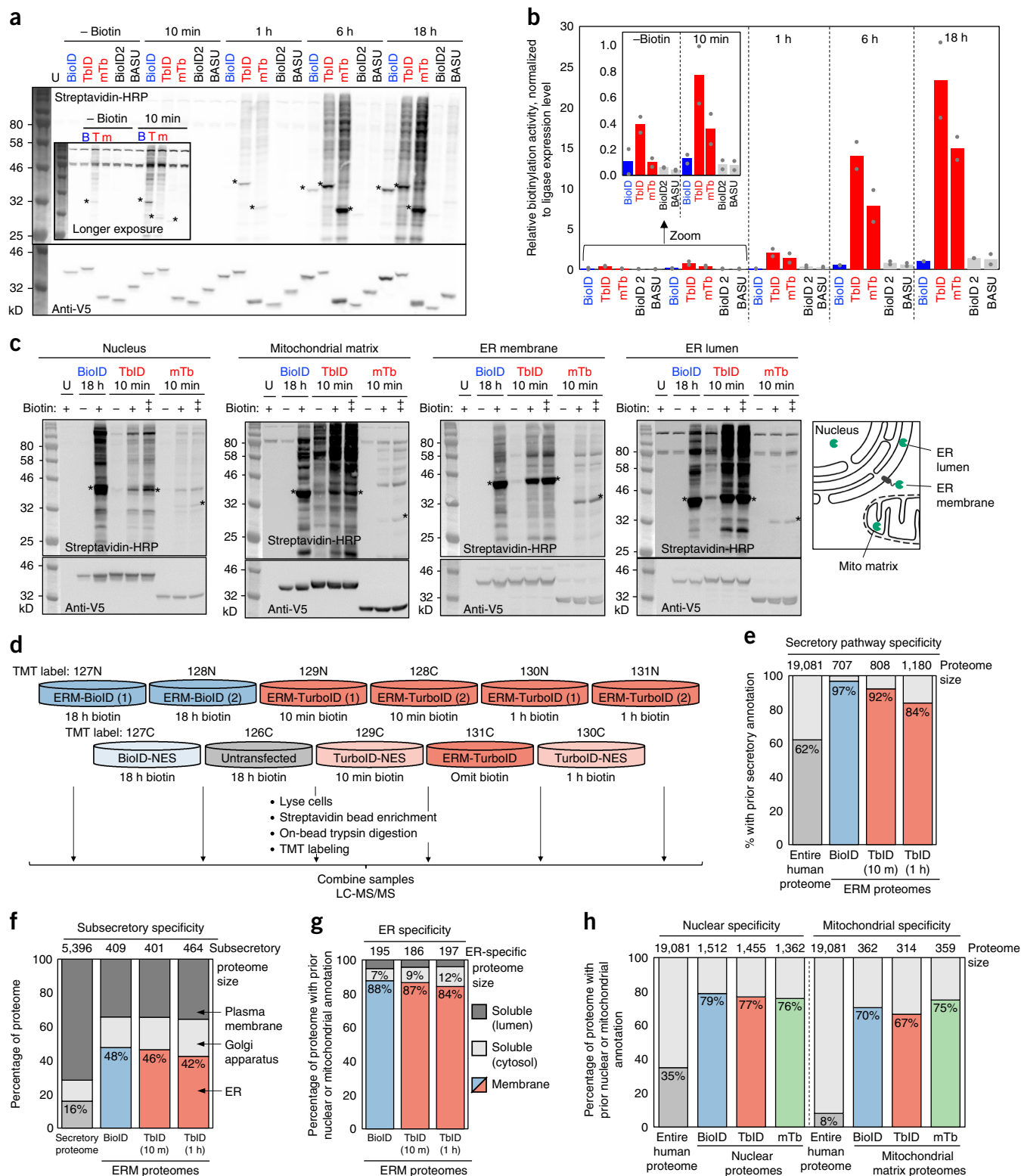
While we observed background labeling by TurboID in adult biotin-depleted worms (Fig. 3i), similar to our observations in

Figure 2 Characterization of TurboID and miniTurbo in mammalian cells. (a) Comparison of TurboID and miniTurbo to three other promiscuous ligases (BioID⁵, BioID2²⁶, and BASU²⁷) in the cytosol of HEK 293T cells. Here, 500 μ M exogenous biotin was used for labeling, whereas 50 μ M was used in Supplementary Figure 6c–e. Streptavidin-HRP blotting detects promiscuously biotinylated proteins, and anti-V5 blotting detects ligase expression. U, untransfected. Asterisks denote ligase self-biotinylation bands. This experiment was performed twice with similar results. All results shown here were performed side by side in a single experiment. (b) Quantitation of experiment in a. For shorter time points (–biotin and 10 min), we used a longer-exposure image of the same blot, shown in Supplementary Figure 6a; for longer time points (1 h, 6 h, 18 h), we used a shorter-exposure image of the blot in a, shown in Supplementary Figure 6b. Quantitation performed as in Figure 1g. Gray dots indicate quantitation of signal intensity from each replicate, colored bars indicate mean signal tyramide signal amplification (TSA) intensity calculated from the two replicates. (c) Comparison of promiscuous ligases in multiple HEK organelles. Each ligase was fused to a peptide targeting sequence (Supplementary Table 8) directing them to the locations indicated in the scheme at right. BioID samples were treated with 50 μ M biotin for 18 h. TurboID and miniTurbo samples were labeled for 10 min with 50 (+) or 500 (++) μ M biotin. U, untransfected. Asterisks denote ligase self-biotinylation. This experiment was performed five times for nuclear constructs, three times for mitochondrial constructs, four times for ER membrane constructs, and twice for ER lumen constructs with similar results. (d) MS-based proteomic experiment comparing TurboID and BioID on the ER membrane (ERM), facing cytosol. Experimental design and labeling conditions. Ligase fusion constructs were stably expressed in HEK 293T. BioID samples were treated with 50 μ M biotin for 18 h, while TurboID samples were treated with 500 μ M biotin for 10 min or 1 h. After labeling, cells were lysed and biotinylated proteins were enriched with streptavidin beads, digested to peptides, and conjugated to TMT (tandem mass tag) labels. All 11 samples were then combined and analyzed by LC-MS/MS. Proteomic lists in Supplementary Table 5; further analysis of proteome data in Supplementary Figure 9. This experiment was performed once with two replicates per condition. All results shown here are from two replicates performed within one experiment. (e) Specificity analysis for proteomic data sets derived from experiment in d. Size of each ERM proteome at top. Bars show percentage of each proteome with prior secretory pathway annotation, according to GOCC, Phobius, human protein atlas, human plasma proteome database, and literature (Supplementary Table 2). (f) Same as e, except for each ERM proteome, we analyze the subset with ER, Golgi, or plasma membrane annotation. Annotations from GOCC were assigned in the priority order: ER > Golgi > plasma membrane (Supplementary Table 2). (g) Breakdown of ER proteins enriched by TurboID and BioID, by transmembrane or soluble. Soluble proteins were further divided into luminal or cytosol-facing. Annotations obtained from GOCC, UniProt, TMHMM, and literature (Supplementary Table 2). (h) Characterization of nuclear and mitochondrial matrix proteomes obtained via BioID (18 h), TurboID (10 min), and miniTurbo (10 min)-catalyzed labeling. Proteome sizes across top. Bars show fraction of each nuclear (left) or mitochondrial (right) proteome with prior nuclear or mitochondrial annotation, according to GOCC, MitoCarta, or literature (Supplementary Tables 3 and 4). Design of proteomic experiment shown in Supplementary Figure 10a, proteomic lists in Supplementary Tables 6 and 7; further analysis of proteome data in Supplementary Figure 10.

flies and mammalian cell culture, we found that miniTurbo, but not TurboID, gave some background labeling in biotin-depleted worm embryos at stage 2 (Fig. 3k and Supplementary Fig. 15a). We also assessed viability and developmental timing, and did not observe decreased survival in worms expressing any of the three

ligases in intestinal cells; however, developmental delay was evident in worms expressing TurboID (Supplementary Fig. 16 and Supplementary Note 5).

In summary, we have performed yeast-display-based directed evolution, incorporating TSA signal amplification, reductive removal of



ligases, and negative selections, to generate two new ligases for PL applications: TurboID and miniTurbo. TurboID is the most active, and should be used when the priority is to maximize biotinylation yield and sensitivity and/or recovery. However, in many contexts, we observe a small degree of labeling before exogenous biotin is supplied, indicating that TurboID can utilize the low levels of biotin present in cells and/or organisms grown in typical biotin-containing media or food. Hence, if the priority is to precisely define the labeling time window, miniTurbo may be preferable to TurboID. Though 1.5- to twofold less active than TurboID, miniTurbo gives much less background in the biotin-omitted condition, and it is also 20% smaller (28 vs. 35 kD), which may reduce interference with fusion protein trafficking and function. Yet another factor to consider when choosing a ligase for PL is ligase stability. Our results indicate that miniTurbo is less stable than TurboID (likely due to removal of its N-terminal domain), resulting in lower expression levels in the adult worm intestine and adult fly, for example. miniTurbo also exhibits biotin-dependent stability, similar to BioID (e.g., see anti-V5 western blots in Fig. 2a).

Up to now, *in vivo* applications of PL have required very long labeling times^{24,34} or extensive genetic or manual manipulation^{35–37} to deliver chemical substrates to relevant cells. TurboID and miniTurbo offer facile substrate delivery and rapid labeling *in vivo*. In addition to increased catalytic efficiency, we believe that the temperature-activity profiles of TurboID and miniTurbo help to explain their superior performance to BioID *in vivo*. Whereas BioID is derived from *E. coli* (37 °C), TurboID and miniTurbo were evolved in yeast (30 °C). Flies grow at 25 °C, while worms are typically grown at 20 °C.

Our toxicity analyses in flies, worms, and mammalian cell culture (Supplementary Figs. 13, 14 and 16) do suggest some necessary precautions when using TurboID and miniTurbo *in vivo*. First, if

TurboID is expressed ubiquitously, it can sequester endogenous biotin and cause toxicity; the solution is to supplement animals with exogenous biotin. Second, users should empirically optimize the *in vivo* labeling time window, and use the shortest labeling time that produces sufficient biotinylated material for analysis. Longer-than-necessary labeling can cause toxicity via chronic biotinylation of endogenous proteomes, and/or degrade spatial specificity due to saturation of proximal labeling sites (Fig. 2e).

METHODS

Methods, including statements of data availability and any associated accession codes and references, are available in the [online version of the paper](#).

Note: Any Supplementary Information and Source Data files are available in the online version of the paper.

ACKNOWLEDGMENTS

FACS was performed at the Koch Institute Flow Cytometry Core (MIT) and Stanford Shared FACS Facility. S. Han (Stanford) synthesized neutravidin-AlexaFluor647. S. Ax (Stanford) cloned the cell surface TurboID and miniTurbo constructs. We are grateful to I. Droujinine (Harvard) for advice on biotin labeling in *D. melanogaster*. Biotin auxotrophic *E. coli* MG1655bioB:kan was kindly donated by J. Cronan (University of Illinois). This work was supported by NIH R01-CA186568 (to A.Y.T.), Howard Hughes Medical Institute Collaborative Innovation Award (to A.Y.T., S.C., and N.P.), and NIH New Innovator Award DP2GM119136 (to J.L.F.). T.C.B. was supported by Dow Graduate Research and Lester Wolfe Fellowships. J.A.B. was supported by a Damon Runyon Post-Doctoral Fellowship. A.D.S. was supported by NIH Training Grant 2T32GM007276.

AUTHOR CONTRIBUTIONS

T.C.B. and A.Y.T. designed the research and analyzed all the data except those noted. T.C.B. performed all experiments except those noted. T.C.B., A.Y.T., N.D.U., and S.A.C. designed the proteomics experiments. T.C.B. prepared the proteomic samples. N.D.U. and T.S. processed the proteomic samples and performed mass

Figure 3 TurboID and miniTurbo in flies, worms, and other species. **(a)** Comparison of ligases in yeast. EBY100 *S. cerevisiae* expressing BioID, TurboID, or miniTurbo in the cytosol were treated with 50 μ M biotin for 18 h. Whole cell lysates were blotted with streptavidin-HRP to visualize biotinylated proteins, and anti-V5 antibody to visualize ligase expression. U, untransfected. Asterisks denote ligase self-biotinylation. Bands in untransfected lane are endogenous, naturally biotinylated proteins. This experiment was performed twice with similar results. **(b)** Comparison of ligases in *E. coli*. Ligases, fused at their N-terminal ends to His6-maltose binding protein, were expressed in the cytosol of BL21 *E. coli* and 50 μ M exogenous biotin was added for 18 h. Whole cell lysates were analyzed as in **a**. This experiment was performed twice with similar results. **(c–g)** Comparison of ligases in flies. **(c)** Scheme for tissue-specific expression of ligases in the wing disc of *D. melanogaster*. *ptc-Gal4* induces ligase expression in a strip of cells within the wing imaginal disc that borders the anterior/posterior compartments. **(d)** Imaging of larval wing discs after 5 d of growth on biotin-containing food. Biotinylated proteins are detected by staining with streptavidin-AlexaFluor555, and ligase expression is detected by anti-V5 staining. Panels show the pouch region of the wing disc, indicated by the dashed line in **c**. Scale bar, 40 μ m. Each experimental condition has at least three technical replicates; one representative image is shown. This experiment was independently repeated two times with similar results. **(e)** Quantitation of streptavidin-AlexaFluor555 signal intensities in **d**. Error bars, s.e.m. Average fold-change shown as text above bars. Sample size values (*n*) from left column to right: 5, 6, 3. **(f)** Scheme for ubiquitous expression of ligases in flies, at all developmental time points, via the *act-Gal4* driver. **(g)** Western blotting of fly lysates prepared as in **f**. Biotinylated proteins detected by blotting with streptavidin-HRP, ligase expression detected by anti-V5 blotting. In control sample, *act-Gal4* drives expression of *UAS-luciferase*. Bands in control lanes are endogenous, naturally biotinylated proteins. This experiment was performed twice with similar results. **(h–k)** Comparison of ligases in worms. **(h)** Scheme for tissue-specific expression of ligases in *C. elegans* intestine via *ges-1p* promoter. Transgenic strains are fed either biotin-producing *E. coli* OP50 (biotin+), or biotin-auxotrophic *E. coli* MG1655bioB:kan (biotin–). Promoter *ges-1p* drives ligase expression ~150 min after the first cell cleavage. **(i)** Adult worms prepared as in **h** were shifted to 25 °C for one generation, then lysed and analyzed by western blotting. Control worms (N2) do not express ligase. Anti-HA antibody detects ligase expression. Streptavidin-IRDye detects biotinylated proteins. This experiment was performed five times (*n* = 5). In biotin+ conditions, BioID biotinylation activity was undetectable and TurboID gave robust biotinylation signal (*n* = 5/5). Despite high activity detected in embryos (see **j,k**), we only detected low levels of biotinylation by miniTurbo in adults (*n* = 2/5), likely due to low ligase expression. **(j)** Representative images of bean stage (stage 1) worm embryos from **h**. See **Supplementary Figure 15a** for representative images of comma-stage worm embryos (stage 2). Embryos were fixed and stained with streptavidin-AF488 to detect biotinylated proteins, and anti-HA antibody to detect ligase expression. Intestine is outlined by a white dotted line. Scale bar, 10 μ m. **(k)** Quantitation of streptavidin-AF488 signal acquired from staining of embryonic stages 1 and 2 shown in **j** and **Supplementary Figure 15a**. Mean streptavidin pixel intensities for each embryo assessed are plotted for BioID (B), TurboID (T), and miniTurbo (mT). Two independent transgenic lines for BioID and TurboID and one for miniTurbo were assessed. Number of embryos imaged (*n*) from left to right: 26, 18, 11, 16, 25, 8, 19, 23, 14, 14, 23, 9. Statistical significance via Mann–Whitney *U* test (two-sided). ****P* ≤ 0.0001, ***P* ≤ 0.001, **P* ≤ 0.01. Pink asterisks indicate significance of pairwise comparisons between biotin– and corresponding biotin+–treated embryos. Mean (reported in **Supplementary Fig. 15b**) is shown as a black horizontal line for each condition, and error bars indicate s.e.m. Note that the streptavidin-AF488 pixel intensities for miniTurbo are an underrepresentation of the signal as camera exposure settings were lowered to avoid pixel saturation (see **Methods**). See **Supplementary Figure 15** for more details.

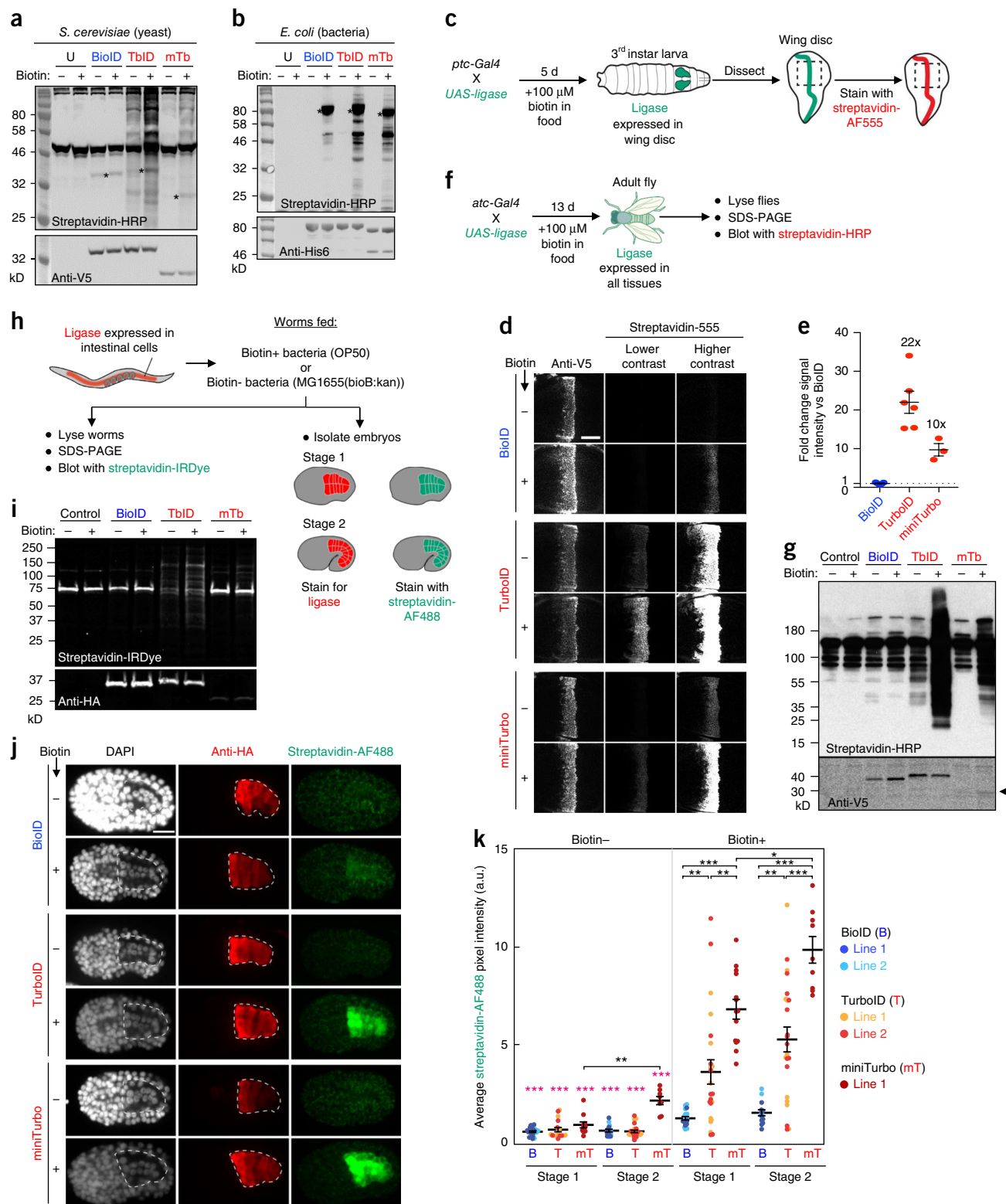
spectrometry. J.A.B. performed *D. melanogaster* experiments. J.A.B. and N.P. analyzed *D. melanogaster* data. T.C.B., A.Y.T., A.D.S., and J.L.F. designed the *C. elegans* experiments. A.D.S. performed *C. elegans* experiments. A.D.S. and J.L.F. analyzed *C. elegans* data.

COMPETING INTERESTS

A.Y.T. and T.C.B. have filed a patent application covering some aspects of this work.

Reprints and permissions information is available online at <http://www.nature.com/reprints/index.html>. Publisher's note: Springer Nature remains neutral with regard to jurisdictional claims in published maps and institutional affiliations.

- Kim, D.I. & Roux, K.J. Filling the void: proximity-based labeling of proteins in living cells. *Trends Cell Biol.* **26**, 804–817 (2016).
- Rhee, H.-W. *et al.* Proteomic mapping of mitochondria in living cells via spatially restricted enzymatic tagging. *Science* **339**, 1328–1331 (2013).



3. Lam, S.S. *et al.* Directed evolution of APEX2 for electron microscopy and proximity labeling. *Nat. Methods* **12**, 51–54 (2015).
4. Choi-Rhee, E., Schulman, H. & Cronan, J.E. Promiscuous protein biotinylation by *Escherichia coli* biotin protein ligase. *Protein Sci.* **13**, 3043–3050 (2004).
5. Roux, K.J., Kim, D.I., Raida, M. & Burke, B. A promiscuous biotin ligase fusion protein identifies proximal and interacting proteins in mammalian cells. *J. Cell Biol.* **196**, 801–810 (2012).
6. Paek, J. *et al.* Multidimensional tracking of GPCR signaling via peroxidase-catalyzed proximity labeling. *Cell* **169**, 338–349.e11 (2017).
7. Lobingier, B.T. *et al.* An approach to spatiotemporally resolve protein interaction networks in living cells. *Cell* **169**, 350–360.e12 (2017).
8. Kaewsapsak, P., Shechner, D.M., Mallard, W., Rinn, J.L. & Ting, A.Y. Live-cell mapping of organelle-associated RNAs via proximity biotinylation combined with protein-RNA crosslinking. *eLife* **6**, e29224 (2017).
9. Martell, J.D. *et al.* Engineered ascorbate peroxidase as a genetically encoded reporter for electron microscopy. *Nat. Biotechnol.* **30**, 1143–1148 (2012).
10. Gupta, G.D. *et al.* a dynamic protein interaction landscape of the human centrosome-cilium interface. *Cell* **163**, 1484–1499 (2015).
11. Kim, D.I. *et al.* Probing nuclear pore complex architecture with proximity-dependent biotinylation. *Proc. Natl. Acad. Sci. USA* **111**, E2453–E2461 (2014).
12. Lin, Q. *et al.* Screening of proximal and interacting proteins in rice protoplasts by proximity-dependent biotinylation. *Front. Plant Sci.* **8**, 749 (2017).
13. Morriswood, B. *et al.* Novel bilobe components in *Trypanosoma brucei* identified using proximity-dependent biotinylation. *Eukaryot. Cell* **12**, 356–367 (2013).
14. Chen, A.L. *et al.* Novel components of the *Toxoplasma* inner membrane complex revealed by BioID. *MBio* **6**, e02357–e14 (2015).
15. Nadipuram, S.M. *et al.* *In vivo* biotinylation of the *toxoplasma* parasitophorous vacuole reveals novel dense granule proteins important for parasite growth and pathogenesis. *MBio* **7**, e00808–16 (2016).
16. Chen, A.L. *et al.* Novel insights into the composition and function of the *Toxoplasma* IMC sutures. *Cell. Microbiol.* **19**, e12678 (2017).
17. Long, S. *et al.* Calmodulin-like proteins localized to the conoid regulate motility and cell invasion by *Toxoplasma gondii*. *PLoS Pathog.* **13**, e1006379 (2017).
18. Zhou, Q., Hu, H. & Li, Z. An EF-hand-containing protein in *Trypanosoma brucei* regulates cytokinesis initiation by maintaining the stability of the cytokinesis initiation factor C1F1. *J. Biol. Chem.* **291**, 14395–14409 (2016).
19. Dang, H.Q. *et al.* Proximity interactions among basal body components in *Trypanosoma brucei* identify novel regulators of basal body biogenesis and inheritance. *MBio* **8**, e02120–16 (2017).
20. Kehr, J., Frischknecht, F. & Mair, G.R. Proteomic analysis of the *Plasmodium berghei* gametocyte egressome and vesicular BioID of osmiophilic body proteins identifies merozoite TRAP-like protein (MTRAP) as an essential factor for parasite transmission. *Mol. Cell. Proteomics* **15**, 2852–2862 (2016).
21. Gaji, R.Y. *et al.* Phosphorylation of a myosin motor by TgCDPK3 facilitates rapid initiation of motility during *Toxoplasma gondii* egress. *PLoS Pathog.* **11**, e1005268 (2015).
22. Batsios, P., Ren, X., Baumann, O., Laroche, D.A. & Gräf, R. Src1 is a protein of the inner nuclear membrane interacting with the *Dictyostelium* Lamin NE81. *Cells* **5**, 13 (2016).
23. Meyer, I. *et al.* CP39, CP75 and CP91 are major structural components of the *Dictyostelium* centrosome's core structure. *Eur. J. Cell Biol.* **96**, 119–130 (2017).
24. Uezu, A. *et al.* Identification of an elaborate complex mediating postsynaptic inhibition. *Science* **353**, 1123–1129 (2016).
25. Opitz, N. *et al.* Capturing the Ascl1p/receptor for activated C kinase 1 (RACK1) microenvironment at the head region of the 40S ribosome with quantitative BioID in yeast. *Mol. Cell. Proteomics* **16**, 2199–2218 (2017).
26. Kim, D.I. *et al.* An improved smaller biotin ligase for BioID proximity labeling. *Mol. Biol. Cell* **27**, 1188–1196 (2016).
27. Ramanathan, M. *et al.* RNA-protein interaction detection in living cells. *Nat. Methods* **15**, 207–212 (2018).
28. Birendra, K.C. *et al.* VRK2A is an A-type lamin-dependent nuclear envelope kinase that phosphorylates BAF. *Mol. Biol. Cell* **28**, 2241–2250 (2017).
29. Redwine, W.B. *et al.* The human cytoplasmic dynein interactome reveals novel activators of motility. *eLife* **6**, e28257 (2017).
30. Jung, E.M. *et al.* Arid1b haploinsufficiency disrupts cortical interneuron development and mouse behavior. *Nat. Neurosci.* **20**, 1694–1707 (2017).
31. Martell, J.D. *et al.* A split horseradish peroxidase for the detection of intercellular protein-protein interactions and sensitive visualization of synapses. *Nat. Biotechnol.* **34**, 774–780 (2016).
32. Bobrow, M.N., Harris, T.D., Shaughnessy, K.J. & Litt, G.J. Catalyzed reporter deposition, a novel method of signal amplification. Application to immunoassays. *J. Immunol. Methods* **125**, 279–285 (1989).
33. Hung, V. *et al.* Proteomic mapping of cytosol-facing outer mitochondrial and ER membranes in living human cells by proximity biotinylation. *eLife* **6**, e24463 (2017).
34. Dingar, D. *et al.* BioID identifies novel c-MYC interacting partners in cultured cells and xenograft tumors. *J. Proteomics* **118**, 95–111 (2015).
35. Reinke, A.W., Balla, K.M., Bennett, E.J. & Troemel, E.R. Identification of microsporidia host-exposed proteins reveals a repertoire of rapidly evolving proteins. *Nat. Commun.* **8**, 14023 (2017).
36. Reinke, A.W., Mak, R., Troemel, E.R. & Bennett, E.J. *In vivo* mapping of tissue- and subcellular-specific proteomes in *Caenorhabditis elegans*. *Sci. Adv.* **3**, e1602426 (2017).
37. Chen, C.-L. Proteomic mapping in live *Drosophila* tissues using an engineered ascorbate peroxidase. *Proc. Natl. Acad. Sci. USA* **112**, 12093–12098 (2015).

ONLINE METHODS

Cloning. See **Supplementary Table 8** for a list of genetic constructs used in this study, with detailed description of construct designs, linker orientations, epitope tags, and signal sequence identities. All ligase variants were derived from *E. coli* biotin protein ligase, have the residue A146 deleted to suppress dimerization³⁸, and are codon optimized for expression in mammalian cells. For cloning, PCR fragments were amplified using Q5 polymerase (New England BioLabs (NEB)). The vectors were double-digested using standard enzymatic restriction digest and ligated to gel purified PCR products by T4 DNA ligation or Gibson assembly. Ligated plasmid products were introduced by heat shock transformation into competent XL1-Blue bacteria. Ligase mutants were either generated using QuikChange mutagenesis (Stratagene) or isolated from individual yeast clones and transferred to mammalian expression vectors using standard cloning techniques.

Yeast cell culture. For yeast-display (**Fig. 1c,e** and **Supplementary Figs. 3** and **4a**), *S. cerevisiae* strain EBY100 was cultured according to previously published protocols³⁹. Cells were propagated at 30 °C in synthetic dextrose plus casein amino acid (SDCAA, 'regular') medium supplemented with tryptophan (20 mg/L). Yeast cells were transformed with the yeast-display plasmid pCTCON2³⁹ using the Frozen E-Z Yeast Transformation II kit (Zymo) according to manufacturer protocols. Transformed cells containing the *TRP1* gene were selected on SDCAA plates and propagated in SDCAA medium at 30 °C. Protein expression was induced by inoculating saturated yeast culture into 10% SD/GCAA (SDCAA medium with 90% of dextrose replaced with galactose), or into "biotin-depleted" medium⁴⁰ (1.7 g/L YNB-Biotin (Sunrise Science Products), 5 g/L ammonium sulfate, 2 g/L dextrose, 18 g/L galactose, complete amino acids, 0.125 ng/mL d-biotin), at a 1:100–1000 dilution and incubating at 30 °C for 18–24 h.

Generation of ligase libraries for yeast display. Libraries of ligase mutants were generated by error-prone PCR according to published protocols⁴¹. 150 ng of the template ligase in vector pCTCON2 (ref. 41) was amplified for 10–20 rounds with 0.4 μM forward and reverse primers:

F: 5'-CTAGTGGTGGAGGAGGCTCTGGTGGAGGCGGTAGCGGAGCGCGAGGGTCCGCTAGC-3'

R: 5'-TATCAGATCTCGAGCTATTACAAGTCTCTCAGAAATAAGCTTTTGTTCCGATCC-3' and 2 mM MgCl₂, 5 units of *Taq* polymerase (NEB), and 2–20 μM each of the mutagenic nucleotide analogs 8-oxo-2'-deoxyguanosine-5'-triphosphate (8-oxo-dGTP) and 2'-deoxy-P-nucleoside-5'-triphosphate (dPTP). The PCR products were then gel purified and reamplified for another 30 cycles under normal PCR conditions using:

F: 5'-CAAGGTCTGCAGGCTAGTGGTGGAGGAGGCTCTGGTG-3'

R: 5'-CTACACTGTTGTTATCAGATCTCGAGCTATTACAAGTC-3'.

The inserts were then electroporated into electrocompetent *S. cerevisiae* EBY100 (ref. 41) with the BamHI-NheI linearized pCTCON2 vector (10 μg insert/1 μg vector) backbone. The electroporated cultures were rescued in 2 mL yeast extract peptone dextrose (YPD) complete medium⁴¹ for 1 h at 30 °C with no shaking. Cells were vortexed briefly, and 1.99 mL of the rescued cell suspension was transferred to 100 mL of SDCAA medium supplemented with 50 units/mL penicillin and 50 μg/mL streptomycin and grown for 2 days at 30 °C. The remaining 10 μL of the rescued cell suspension was diluted 100×, 1000×, 10000×, and 100000×; 20 μL of each dilution was plated on SDCAA plates and incubated at 30 °C for 3 days. After 3 days, each colony observed in the 100×, 1000×, 10000×, or 100000× segments of plates will correspond to 10⁴, 10⁵, 10⁶, or 10⁷ transformants in the library, respectively.

General methods for yeast display-based directed evolution. For each round of evolution (**Supplementary Fig. 3**), we input 10-fold more yeast cells than the estimated library size. For the first round, library size was estimated by the transformation efficiency of the initial ligase library. For subsequent rounds, library size was taken to be the number of yeast cells collected during the previous sort. Ligase protein expression was induced by inoculating saturated yeast culture into 10% SD/GCAA or biotin-depleted medium at a 1:1000 dilution and incubating at 30 °C for 18–24 h. However, when inducing yeast populations with high diversity, for example the initial libraries, saturated

yeast cultures were diluted at as high as 1:100 dilution into the appropriate induction media in order to conserve media.

For samples biotin labeled for 18 h, yeast were induced in 10% SD/GCAA or biotin-depleted medium supplemented with 50 μM biotin, 1 mM ATP, and 5 mM MgCl₂ at 30 °C for 20–24 h (to allow time for protein expression and ensure labeling occurs for at least 18 h). For samples labeled for shorter time periods, yeast were induced in 10% SD/GCAA or biotin-depleted medium for 18 h at 30 °C (no biotin), then supplemented with 50 μM biotin, 1 mM ATP, and 5 mM MgCl₂ for the labeling times indicated. For 'omit biotin' samples, yeast were induced in 10% SD/GCAA or biotin-depleted medium at 30 °C for 18–24 h. After labeling, approximately 5 million cells (assuming 1 OD₆₀₀ ≈ 3 × 10⁷ cells⁴²) were pelleted at 5000×g for 30 s at 4 °C and washed five times with 1 mL PBS (phosphate buffered saline) + 0.5% bovine serum albumin (BSA; 1 mg/mL) (PBS-B).

For tyramide signal amplification³² (TSA, **Supplementary Fig. 3b**), yeast cells were incubated in 50 μL PBS-B + 1:100 streptavidin-horseradish peroxidase (HRP) for 1 h at 4 °C, then washed three times with 1 mL PBS-B. HRP labeling was performed by incubating yeast in 750 μL PBS-B with 50 μM biotin-phenol and 1 mM H₂O₂ for 1 min at room temperature. The reaction was quenched by adding 750 μL PBS-B + 20 mM sodium ascorbate and 10 mM Trolox followed by rapid mixing via inversion. Cells were then washed two times with 1 mL PBS-B + 10 mM sodium ascorbate and 5 mM Trolox, and once with 1 mL PBS-B. For removal of ligase proteins via TCEP reduction (**Supplementary Fig. 3c**), yeast were incubated in 500 μL PBS-B + 2 mM TCEP at 30 °C for 90 min, then washed four times with 1 mL PBS-B.

For biotin and epitope tag detection, yeast cells were then incubated in 50 μL PBS-B + 1:400 chicken anti-myc and 1:50 rabbit anti-biotin (when detecting biotinylated proteins with anti-biotin antibody) for 1 h at 4 °C, then washed three times with 1 mL PBS-B. Yeast cells were then incubated in 50 μL PBS-B + 1:200 Alexa Fluor 647 (AF647) goat anti-chicken IgG and 1:50 phycoerythrin (PE) goat anti-rabbit IgG (when detecting biotinylated proteins with anti-biotin antibody) or streptavidin-PE (when detecting biotinylated proteins with streptavidin) for 1 h at 4 °C, then washed three times with 1 mL PBS-B for FACS analysis. Refer to **Supplementary Table 9** for a list of antibodies used in this study.

For two-dimensional FACS sorting, samples were resuspended in PBS-B at a maximal concentration of 100 million cells/mL and sorted on a BD FACS Aria II cell sorter (BD Biosciences) with the appropriate lasers and emission filters (561 nm excitation laser and 582/15 emission filter for PE, 640 nm excitation laser and 670/30 emission filter for AF647). To analyze and sort single yeast cells, cells were plotted by a forward-scatter area (FSC-A) and side-scatter area (SSC-A) and a gate was drawn around cells clustered between 10⁴–10⁵ FSC-A, 10³–10⁵ SSC-A to give population P1 (**Supplementary Fig. 3i**). Cells from population P1 were then plotted by side-scatter width (SSC-W) and side-scatter height (SSC-H) and a gate was drawn around cells clustered between 10–100 SSC-W and 10³–10⁵ SSC-H to give population P2 (**Supplementary Fig. 3i**). Cells from population P2 were then plotted by forward-scatter width (FSC-W) and forward-scatter height (FSC-H) and a gate was drawn around cells clustered between 10–100 FSC-W and 10³–10⁵ FSC-H to give population P3 (**Supplementary Fig. 3i**). Population P3 often represented >90% of the total population analyzed.

From population P3, gates were drawn to collect yeast with the highest activity/expression ratio, i.e., positive for AF647 signal that also had high PE signal (**Supplementary Fig. 3i**). For TCEP treated samples, gates were drawn to collect yeast with high PE signal and no AF647 signal above background (**Supplementary Fig. 3i**). For negative selections (**Supplementary Fig. 3f**), gates were drawn to collect yeast with AF647 signal and no PE signal above background (**Supplementary Fig. 3i**). After sorting, yeast were collected in SDCAA medium containing 1% penicillin-streptomycin and incubated at 30 °C for 24 h. 1 mL of the growing culture was removed for DNA extraction using the ZymoPrep yeast Plasmid Miniprep II (Zymo Research) kit according to manufacturer protocols (using 6 μL zymolyase, vigorously vortex after lysis), and at least ten-fold excess of the number of cells retained during sorting were propagated in SDCAA + 1% pen-strep to ensure oversampling (yeast cells were passaged in this manner at least two times prior to the next round of selection). To analyze yeast populations and clones by FACS (**Fig. 1c,e**; **Supplementary Figs. 3** and **4a**), yeast samples were prepared on a small scale (1 mL cultures) as described above and analyzed on a BD Accuri flow cytometer (BD Biosciences). BD FACSDIVA software was used to analyze

all data from FACS sorting and analysis. Summaries of all yeast-display directed evolution and resulting mutants are shown in **Figure 1e**; **Supplementary Figures 3 and 4**, and **Supplementary Table 1**, and are described in detail in the 'Directed evolution of TurboID and miniTurbo' sections below.

Directed evolution of TurboID and miniTurbo: generation 1. For the first round of evolution (**Supplementary Fig. 3b**), three libraries were generated using BirA-R118S (**Supplementary Table 8**) as the starting template. The three libraries were generated using error prone PCR as described above, using the following conditions to produce varying levels of mutagenesis:

Library 1: 2 μ M 8-oxo-dGTP, 2 μ M dPTP, 10 PCR cycles

Library 2: 2 μ M 8-oxo-dGTP, 2 μ M dPTP, 20 PCR cycles

Library 3: 20 μ M 8-oxo-dGTP, 20 μ M dPTP, 10 PCR cycles

The library sizes (approximated by number of transformants as described above), were 1.4×10^7 for Library 1, 1.7×10^7 for Library 2, and 8×10^6 for Library 3. FACS analysis of the three libraries showed robust expression and wide range of activities for Library 1 and Library 2, however Library 3 showed poor expression and no activity. Sequencing of 24 clones in Library 1 revealed an average of 1.5 amino acid changes per ligase gene. Sequencing of 24 clones in Library 2 revealed an average of 2.4 amino acid changes per ligase gene.

Library 1 and Library 2 were combined and used as the initial population for the first round of selections. This combined library was induced as described above, supplemented with 50 μ M biotin, 1 mM ATP, and 5 mM MgCl_2 , for 24 h. From this culture, approximately 5×10^8 cells were prepared for sorting (assuming $1 \text{ OD}_{600} \approx 3 \times 10^7$ cells⁴²) as described above with TSA treatment (**Supplementary Fig. 3b**). 6.24×10^7 cells were sorted by FACS. A square gate that collected cells positive for both anti-myc and streptavidin (conjugated to fluorophores, see **Supplementary Table 9**) was drawn, and approximately 2.5×10^6 cells were collected (4%) to give population E1-R1.

Population E1-R1 was passed twice, and analyzed by FACS side-by-side with the original combined library and BirA-R118S to ensure the sort was successful (resulting population still had expression and had higher or equivalent activity). Sequencing of 24 clones from E1-R1 revealed an average of 1.5 mutations per ligase gene. Population E1-R1 was induced, supplemented with 50 μ M biotin, 1 mM ATP, and 5 mM MgCl_2 , for 24 h. From this culture, approximately 10-fold excess (i.e. $>2.5 \times 10^7$) cells were prepared for sorting with TSA treatment. A square gate that collected cells positive for both anti-myc and streptavidin was drawn, and approximately 3.8% of cells were collected to give population E1-R2.

Population E1-R2 was passed twice, and analyzed by FACS side-by-side with previous rounds and BirA-R118S. Sequencing of 24 clones from E1-R2 revealed an average of 1.5 mutations per ligase gene. Population E1-R2 was induced for ~18 h then supplemented with 50 μ M biotin, 1 mM ATP, and 5 mM MgCl_2 for 6 hours. From this culture, approximately 10-fold excess cells were prepared for sorting with TSA treatment. A square gate that collected cells positive for both anti-myc and streptavidin was drawn, and approximately 0.7% of cells were collected to give population E1-R3.

Population E1-R3 was passed twice, and analyzed by FACS side-by-side with previous rounds and BirA-R118S. Population E1-R3 was induced for ~18 h then supplemented with 50 μ M biotin, 1 mM ATP, and 5 mM MgCl_2 for 6 hours. From this culture, approximately 10-fold excess cells were prepared for sorting with TSA treatment. A square gate that collected cells positive for both anti-myc and streptavidin was drawn, and approximately 2.4% of cells were collected to give population E1-R4.

Population E1-R4 was passed twice, and analyzed by FACS side-by-side with previous rounds and BirA-R118S. Population E1-R4 was induced for ~18 h then supplemented with 50 μ M biotin, 1 mM ATP, and 5 mM MgCl_2 for 3 hours. From this culture, approximately 10-fold excess cells were prepared for sorting. A square gate that collected cells positive for both anti-myc and streptavidin was drawn, and approximately 2.6% of cells were collected to give population E1-R5.

Population E1-R5 was passed twice, and analyzed by FACS side-by-side with previous rounds and BirA-R118S. Population E1-R5 was induced for ~18 h then supplemented with 50 μ M biotin, 1 mM ATP, and 5 mM MgCl_2 for 1 h. From this culture, approximately 10-fold excess cells were prepared for sorting. A square gate that collected cells positive for both anti-myc and streptavidin was drawn, and approximately 0.9% of cells were collected to give population E1-R6.

Population E1-R6 was passed twice, and analyzed by FACS side-by-side with previous rounds and BirA-R118S. Sequencing of E1-R6 revealed several mutants with the mutation E313K. Several mutants with and without this mutation were assayed as single clones on the yeast surface, and the most promising mutants, including two with the E313K mutation, were assayed in the mammalian cell cytosol. While neither of the E313K mutants showed significant difference in activity to R118S over 24 h, they both showed very strong self-labeling at shorter time points, e.g. 1 h. The crystal structure of BirA⁴³ shows that this residue points directly into the active site, where a lysine mutation could easily react with the phosphate group of biotin-5'-AMP. We removed this mutation from the two promising clones bearing it and assayed again in the mammalian cell cytosol. One of the mutants, denoted in this study as G1 (**Supplementary Table 1**), displayed significantly higher promiscuous activity than R118S after 24 hours of labeling. Another mutant from the mammalian cell screen, denoted in this study as R6-1 (**Supplementary Table 1**), also displayed significantly higher promiscuous activity than R118S after 24 h of labeling. Both of these mutants, with 4 mutations each, had each of their mutations removed individually and in different combinations. Analysis of the resulting mutants in mammalian cells showed that each mutation was contributing to increased activity relative to R118S observed for R6-1 and G1.

Directed evolution of TurboID and miniTurbo: generation 2. For the second round of evolution (**Supplementary Fig. 3c**), six libraries were generated. Three libraries were made using R6-1 (**Supplementary Tables 1 and 8**) as the starting template, and the three libraries were made using G1 (**Supplementary Tables 1 and 8**) as the starting template, both using error prone PCR with the following conditions:

Library 1: R6-1, 2 μ M 8-oxo-dGTP, 2 μ M dPTP, 10 PCR cycles

Library 2: R6-1, 2 μ M 8-oxo-dGTP, 2 μ M dPTP, 20 PCR cycles

Library 3: R6-1, 20 μ M 8-oxo-dGTP, 20 μ M dPTP, 10 PCR cycles

Library 4: G1, 2 μ M 8-oxo-dGTP, 2 μ M dPTP, 10 PCR cycles

Library 5: G1, 2 μ M 8-oxo-dGTP, 2 μ M dPTP, 20 PCR cycles

Library 6: G1, 20 μ M 8-oxo-dGTP, 20 μ M dPTP, 10 PCR cycles

The library sizes, as calculated by transformation efficiency, were 3.8×10^7 for Library 1, 1.9×10^7 for Library 2, 1.6×10^7 for Library 3, 8×10^7 for Library 4, 3.9×10^7 for Library 5, and 3.9×10^7 for Library 6. FACS analysis of the three libraries showed robust expression and wide range of activities for Libraries 1, 2, 4, and 5, however Libraries 3 and 6 showed poor expression and no activity.

Libraries 1, 2, 4, and 5 were combined and used as the initial population for the first round of selections. This combined library was induced, supplemented with 50 μ M biotin, 1 mM ATP, and 5 mM MgCl_2 , for 24 h. From this culture, approximately 10-fold excess cells were prepared for sorting with TSA treatment. A square gate that collected cells positive for both anti-myc and streptavidin was drawn, and approximately 8.4% of cells were collected to give population E2-R1.

Population E2-R1 was passed twice, and analyzed by FACS side-by-side with the combined library template. Population E2-R1 was induced, supplemented with 50 μ M biotin, 1 mM ATP, and 5 mM MgCl_2 , for 24 h. From this culture, approximately 10-fold excess cells were prepared for sorting with TCEP treatment (**Supplementary Fig. 3c**) followed by TSA treatment. A square gate that collected cells positive for streptavidin but negative for anti-myc was drawn, and approximately 1.2% of cells were collected to give population E2-R2.

Population E2-R2 was passed twice, and analyzed by FACS side-by-side with the combined library template and previous rounds. Population E2-R2 induced, supplemented with 50 μ M biotin, 1 mM ATP, and 5 mM MgCl_2 , for 24 h. From this culture, approximately 10-fold excess cells were prepared for sorting with TSA treatment. A square gate that collected cells positive for both anti-myc and streptavidin was drawn, and approximately 19% of cells were collected to give population E2-R3.

Population E2-R3 was passed twice, and analyzed by FACS side-by-side with previous rounds. Population E2-R3 was induced, supplemented with 50 μ M biotin, 1 mM ATP, and 5 mM MgCl_2 , for 24 h. From this culture, approximately 10-fold excess cells were prepared for sorting. A trapezoidal gate that collected cells positive for both anti-myc and streptavidin, but with high streptavidin/anti-myc ratios, was drawn, and approximately 1.4% of cells

were collected to give population E2-R4. From here on, only trapezoidal gates as described here were used for double-positive selections.

Population E2-R4 was passaged twice, and analyzed by FACS side-by-side with previous rounds. Population E2-R4 was induced for ~18 h, then supplemented with 50 μ M biotin, 1 mM ATP, and 5 mM $MgCl_2$ for 1 h. From this culture, approximately 10-fold excess cells were prepared for sorting. A trapezoidal gate that collected cells positive for both anti-myc and streptavidin was drawn, and approximately 1.1% of cells were collected to give population E2-R5.

Population E2-R5 was passaged twice, and analyzed by FACS side-by-side with the combined library template and previous rounds. Population E2-R5 was induced for ~18 h, then supplemented with 50 μ M biotin, 1 mM ATP, and 5 mM $MgCl_2$ for 6 h. From this culture, approximately 10-fold excess cells were prepared for sorting with TCEP treatment followed by TSA. A square gate that collected cells positive for streptavidin and negative for anti-myc was drawn, and approximately 1.5% of cells were collected to give population E2-R6.

Population E2-R6 was passaged twice, and analyzed by FACS side-by-side with previous rounds and the combined library template. Sequencing of E2-R6 revealed several mutations that appeared in multiple clones. Several of these mutants were assayed as single clones on the yeast surface, however it was found after re-sequencing that many of the most promising mutants had mutated stop codons. After mutating back the stop codons, the mutants were re-assayed on the yeast surface, and the mutants that remained promising were assayed in the mammalian cell cytosol. One of the mutants, denoted in this study as G2 (**Supplementary Table 1**), displayed significantly higher promiscuous activity than R118S, G1 (its template), or any other mutant tested after 1 hour of labeling. G1, with 2 additional mutations relative to G1, had each or both of its mutations removed. Analysis of the resulting mutants in mammalian cells showed that each mutation was contributing to activity boost observed for G2.

Directed evolution of TurboID and miniTurbo: generation 3. For the third round of evolution (**Supplementary Fig. 3d**), three libraries were made using G2 as the starting template (**Supplementary Tables 1 and 8**) using error prone PCR with the following conditions:

Library 1: 2 μ M 8-oxo-dGTP, 2 μ M dPTP, 10 PCR cycles

Library 2: 2 μ M 8-oxo-dGTP, 2 μ M dPTP, 20 PCR cycles

Library 3: 10 μ M 8-oxo-dGTP, 20 μ M dPTP, 10 PCR cycles

The library sizes, as calculated by transformation efficiency, were 3.5×10^8 for Library 1, 3.6×10^7 for Library 2, and 6.8×10^6 for Library 3. FACS analysis of the three libraries showed robust expression and wide range of activities for Library 1 and Library 2, however Library 3 showed weak expression and no activity.

Libraries 1 and 2 were combined and used as the initial population for the first round of selections. This combined library was induced for ~18 h, then supplemented with 50 μ M biotin, 1 mM ATP, and 5 mM $MgCl_2$ for 1 h. From this culture, approximately 10-fold excess cells were prepared for sorting. A trapezoidal gate that collected cells positive for both anti-myc and streptavidin was drawn, and less than 0.1% of cells were collected to give population E3-R1.

Population E3-R1 was passaged twice, and analyzed by FACS side-by-side with G2 and the combined library template. Population E3-R1 was induced for ~18 h, then supplemented with 50 μ M biotin, 1 mM ATP, and 5 mM $MgCl_2$ for 1 h. From this culture, approximately 10-fold excess cells were prepared for sorting. A trapezoidal gate that collected cells positive for both anti-myc and streptavidin was drawn, and 0.15% of cells were collected to give population E3-R2.

Population E3-R2 was passaged twice, and analyzed by FACS side-by-side with G2, the combined library template, and previous rounds. Population E3-R2 was induced for ~18 h, then supplemented with 50 μ M biotin, 1 mM ATP, and 5 mM $MgCl_2$ for 10 min. From this culture, approximately 10-fold excess cells were prepared for sorting. A trapezoidal gate that collected cells positive for both anti-myc and streptavidin was drawn, and less than 0.1% of cells were collected to give population E3-R3.

At E3-R3, it was noted that the population had strong streptavidin signal in the absence of exogenous biotin addition. Sequencing of population E3-R3 revealed that the majority of clones had a large insertion at the 5' of the ligase gene. Removal of this insertion restored biotin dependence, but also resulted

in decreased activity (5-fold less than E3-R3). The library was 'cleaned' by removing this insertion via PCR with primers that restored the wild-type N-terminal sequence, and subjected to one additional round of double-positive selection with 10 minute labeling and 0.1% cells collected. The resulting population was E3-R4.

Population E3-R4 was passaged twice, and analyzed by FACS side-by-side with previous rounds. Sequencing of E3-R4 revealed several mutations that appeared in multiple clones. Several of these mutants were assayed as single clones on the yeast surface, the most promising mutants were assayed in the mammalian cell cytosol. Two mutants had significantly higher activity than the template G2 or any other mutants. The mutations from these mutants were combined in various combinations, resulting in the highest activity mutant, denoted in this study as G3 (**Supplementary Table 1**).

Directed evolution of TurboID and miniTurbo: Generations 4 and 5. G3 was the highest activity mutant found to date, but it also appeared to give labeling even without the addition of exogenous biotin. This was observed in yeast, where this signal proved to be biotin-dependent (**Supplementary Fig. 3e**), and also in the mammalian cytosol (**Fig. 1f, Supplementary Fig. 4b**). From this point, we continued with two evolutionary paths as follows:

In one path, we truncated the N-terminal domain (aa 1-63) of G3 to give G3 Δ (**Supplementary Table 1**). Consistent with literature^{44,45}, this truncation resulted in reduced streptavidin signal when exogenous biotin was omitted (**Supplementary Fig. 3e**). Using G3 Δ as the starting template (**Supplementary Tables 1 and 8**) for another round of evolution (**Supplementary Fig. 3g**), we generated three libraries using error prone PCR with the following conditions:

Library 1: 2 μ M 8-oxo-dGTP, 2 μ M dPTP, 10 PCR cycles

Library 2: 2 μ M 8-oxo-dGTP, 2 μ M dPTP, 20 PCR cycles

Library 3: 4 μ M 8-oxo-dGTP, 2 μ M dPTP, 20 PCR cycles

The library sizes, as calculated by transformation efficiency, were 4.9×10^8 for Library 1, 4.6×10^8 for Library 2, and 3.7×10^8 for Library 3. FACS analysis of the three libraries showed robust expression and wide range of activities for all libraries, therefore all were combined and used for the first round of selections.

This combined library was induced in biotin-depleted media, supplemented with 50 μ M biotin, 1 mM ATP, and 5 mM $MgCl_2$, for 18 h. From this culture, approximately 10-fold excess cells were prepared for sorting with streptavidin. A trapezoidal gate that collected cells positive for both anti-myc and streptavidin was drawn, and 0.1% of cells were collected to give population E4-R1.

Population E4-R1 was passaged twice, and analyzed by FACS side-by-side with G3 Δ and the combined library template. Population E4-R1 was induced for ~18 h in biotin-depleted media, then supplemented with 50 μ M biotin, 1 mM ATP, and 5 mM $MgCl_2$ for 3.5 h. From this culture, approximately 10-fold excess cells were prepared for sorting with anti-biotin antibody. A trapezoidal gate that collected cells positive for both anti-myc and anti-biotin was drawn, and 1% of cells were collected to give population E4-R2.

Population E4-R2 was passaged twice, and analyzed by FACS side-by-side with G3 Δ , the combined library template, and previous rounds. Population E4-R2 was induced for ~18 h in biotin-depleted media, then supplemented with 50 μ M biotin, 1 mM ATP, and 5 mM $MgCl_2$ for 1 h. From this culture, approximately 10-fold excess cells were prepared for sorting with streptavidin. A trapezoidal gate that collected cells positive for both anti-myc and streptavidin was drawn, and 0.2% of cells were collected to give population E4-R3.

Population E4-R3 was passaged twice, and analyzed by FACS side-by-side with G3 Δ , the combined library template, and previous rounds. Population E4-R3 was induced for ~18 h in biotin-depleted media, then supplemented with 50 μ M biotin, 1 mM ATP, and 5 mM $MgCl_2$ for 1 h. From this culture, approximately 10-fold excess cells were prepared for sorting with anti-biotin antibody. A trapezoidal gate that collected cells positive for both anti-myc and anti-biotin was drawn, and 0.1% of cells were collected to give population E4-R4.

Population E4-R4 was passaged twice, and analyzed by FACS side-by-side with G3 Δ , the combined library template, and previous rounds. Population E4-R4 was induced for ~18 h in biotin-depleted media, labeling was omitted for negative selection (**Supplementary Fig. 3f**). From this culture, approximately 10-fold excess cells were prepared for sorting with streptavidin. A square gate that collected cells positive for anti-myc and negative for streptavidin was drawn, and 50% of cells were collected to give population E4-R5.

Population E4-R5 was passaged twice, and analyzed by FACS side-by-side with G3Δ, the combined library template, and previous rounds. Two selections were performed on E4-R5. In the first selection, population E4-R5 was induced for ~18 h in biotin-depleted media, labeling was omitted for negative selection. From this culture, approximately 10-fold excess cells were prepared for sorting with anti-biotin antibody. A square gate that collected cells positive for both anti-myc and anti-biotin was drawn, and 45% of cells were collected to give population E4-R6.1.

In the second selection, population E4-R5 was induced for ~18 h in biotin-depleted media, then supplemented with 50 μM biotin, 1 mM ATP, and 5 mM MgCl₂ for 20 min. From this culture, approximately 10-fold excess cells were prepared for sorting with streptavidin. A trapezoidal gate that collected cells positive for both anti-myc and streptavidin was drawn, and 0.1% of cells were collected to give population E4-R6.2.

One more round of selections was performed on E4-R6.1, which was induced for ~18 h in biotin-depleted media, then supplemented with 50 μM biotin, 1 mM ATP, and 5 mM MgCl₂ for 1 h. From this culture, approximately 10-fold excess cells were prepared for sorting with streptavidin. A trapezoidal gate that collected cells positive for both anti-myc and streptavidin was drawn, and 0.2% of cells were collected to give population E4-R7.

Population E4-R7 was passaged twice, and analyzed by FACS side-by-side with previous rounds. Sequencing of E4-R7 revealed several mutations that appeared in multiple clones. Several of these mutations were assayed as single mutations and in various combinations in the mammalian cytosol. One mutation, K194I, was found to significantly increase activity while not increasing signal exogenous when biotin is omitted. Introducing K194I into G3Δ resulted in miniTurbo (**Supplementary Table 1**).

In a second evolutionary path, we continued with evolving G3 (**Supplementary Fig. 3h**). Two libraries were made using G3 as the starting template (**Supplementary Tables 1 and 8**) using error prone PCR with the following conditions:

Library 1: 2 μM 8-oxo-dGTP, 2 μM dPTP, 10 PCR cycles

Library 2: 2 μM 8-oxo-dGTP, 2 μM dPTP, 20 PCR cycles

The library sizes, as calculated by transformation efficiency, were 2×10^7 for Library 1 and 1.1×10^7 for Library 2. FACS analysis of the libraries showed robust expression and wide range of activities for Library 1 and Library 2.

Libraries 1 and 2 were combined and used as the initial population for the first round of selections. This combined library was induced for ~18 h in biotin-depleted media, then supplemented with 50 μM biotin, 1 mM ATP, and 5 mM MgCl₂ for 10 min. From this culture, approximately 10-fold excess cells were prepared for sorting with anti-biotin antibody (**Supplementary Table 9**) in place of streptavidin. A trapezoidal gate that collected cells positive for both anti-myc and anti-biotin was drawn, and 0.1% of cells were collected to give population E5-R1.

Population E5-R1 was passaged twice, and analyzed by FACS side-by-side with G3 and the combined library template. Population E5-R1 was induced for ~18 h in biotin-depleted media, then supplemented with 50 μM biotin, 1 mM ATP, and 5 mM MgCl₂ for 10 min. From this culture, approximately 10-fold excess cells were prepared for sorting with anti-biotin antibody. A trapezoidal gate that collected cells positive for both anti-myc and anti-biotin was drawn, and 0.1% of cells were collected to give population E5-R2.

Population E5-R2 was passaged twice, and analyzed by FACS side-by-side with G3, the combined library template, and previous rounds. Population E5-R2 was induced for ~18 h in biotin-depleted media, then supplemented with 50 μM biotin, 1 mM ATP, and 5 mM MgCl₂ for 10 min. From this culture, approximately 10-fold excess cells were prepared for sorting with anti-biotin antibody. A trapezoidal gate that collected cells positive for both anti-myc and anti-biotin was drawn, and 1.7% of cells were collected to give population E5-R3.

Population E5-R3 was passaged twice, and analyzed by FACS side-by-side with G3, the combined library template, and previous rounds. Population E5-R3 was induced for ~18 h in regular media, labeling was omitted for negative selection. From this culture, approximately 10-fold excess cells were prepared for sorting with anti-biotin antibody. A square gate that collected cells positive for anti-myc and negative for anti-biotin was drawn, and 34% of cells were collected to give population E5-R4.

Population E5-R4 was passaged twice. FACS analysis side-by-side with G3, the combined library template, and previous rounds showed that the

negative selection that resulted E5-R4 reduced overall activity of the population. Population E5-R4 was induced for ~18 h in biotin depleted media, then supplemented with 50 μM biotin, 1 mM ATP, and 5 mM MgCl₂ for 10 min. From this culture, approximately 10-fold excess cells were prepared for sorting with streptavidin. A trapezoidal gate that collected cells positive for both anti-myc and streptavidin was drawn, and 0.8% of cells were collected to give population E5-R5.

Population E5-R5 was passaged twice, and analyzed by FACS side-by-side with G3, the combined library template, and previous rounds. Population E5-R5 was induced for ~18 h in regular media, labeling was omitted for negative selection. From this culture, approximately 10-fold excess cells were prepared for sorting with anti-biotin antibody. A square gate that collected cells positive for anti-myc and negative for anti-biotin was drawn, and 11.6% of cells were collected to give population E5-R6.

Population E5-R6 was passaged twice, and analyzed by FACS side-by-side with previous rounds. Sequencing of E5-R6 revealed several mutations that appeared in multiple clones. Several of these mutations were assayed as single mutations and in various combinations in the mammalian cytosol. None of the mutations gave dramatic increases in activity, but one mutation M241T, appeared to impart benefits to activity.

Screening of mutations present in E4-R6.2 in the mammalian cell cytosol revealed one mutation, S263P, which boosted activity, but also increased signal when biotin was omitted. This mutation, along with K194I from E4-R7 and M241T from E5-R6, were introduced into G3 to give TurboID (**Supplementary Table 1**). We also tested M241T in miniTurbo, however it was not added because it increased background signal when biotin was omitted.

Mammalian cell culture, transfection, and stable cell line generation. HEK 293T cells from ATCC (passage number <25) were cultured as a monolayer in growth media (either MEM (Cellgro) or a 1:1 DMEM:MEM mixture (Cellgro) supplemented with 10% (w/v) fetal bovine serum (VWR)), 50 units/mL penicillin, and 50 μg/mL streptomycin at 37 °C under 5% CO₂. Mycoplasma testing was not performed before experiments. For confocal imaging experiments, cells were grown on 7 × 7 mm glass coverslips in 48-well plates with 250 μL growth medium. To improve adherence of HEK 293T cells, glass coverslips were pretreated with 50 μg/mL fibronectin (Millipore) in MEM for at least 20 min at 37 °C before cell plating. For Western blotting, cells were grown on polystyrene 6-well plates (Greiner) with 2.5 mL growth medium.

For transient expression (**Fig. 1f, 2c** and **Supplementary Figs. 1, 4b, 5, 10b**, and **14c,d**), cells were typically transfected at approximately 60% confluency using 3.2 μL/mL Lipofectamine2000 (Life Technologies) and 800 ng/mL plasmid in serum-free media (250 μL total volume for 48-wells, 2.5 mL total volume for 6-wells) for 3–4 h, after which time Lipofectamine-containing media was replaced with fresh serum-containing media.

In an attempt to achieve similar expression levels of ligase in the experiment presented in **Figure 2a, b**, **Supplementary Figure 6a, b**, and **Supplementary Figure 7**, cells were transfected at approximately 60% confluency using 1.6 μL/mL Lipofectamine2000 (Life Technologies) in serum-free media with the following amounts of each plasmid (250 μL total volume for 48-wells, 2.5 mL total volume for 6-wells): 160 ng/mL V5-BioID-NES, 80 ng/mL V5-TurboID-NES, 200 ng/mL V5-miniTurbo-NES, 30 ng/mL V5-BioID2-NES, and 1000 ng/mL V5-BASU-NES (**Supplementary Table 8**). After 3–4 h, the Lipofectamine-containing media was replaced with fresh serum-containing media.

In an attempt to achieve similar expression levels of ligase in the experiment presented in **Supplementary Figure 6c–e**, cells were transfected at approximately 60% confluency using 1.6 μL/mL Lipofectamine2000 (Life Technologies) in serum-free media with the following amounts of each plasmid (250 μL total volume for 48-wells, 2.5 mL total volume for 6-wells): 320 ng/mL V5-BioID-NES, 160 ng/mL V5-TurboID-NES, 400 ng/mL V5-miniTurbo-NES, 60 ng/mL V5-BioID2-NES, and 1000 ng/mL V5-BASU-NES (**Supplementary Table 8**). After 3–4 h, the Lipofectamine-containing media was replaced with fresh serum-containing media.

For preparation of lentiviruses, HEK 293T cells in T25 flasks (BioBasic) were transfected at ~60–70% confluency with the lentiviral vector pLX304 containing the gene of interest (2500 ng; **Supplementary Table 8**), and the lentiviral packaging plasmids pVSVG (250 ng; **Supplementary Table 8**) and Δ8.9 (2250 ng; **Supplementary Table 8**) with 30 μL Lipofectamine2000 in

serum-free media for 3 h, after which time the Lipofectamine-containing media was replaced with fresh serum-containing media. Approximately 60 h after transfection, the cell medium containing the lentivirus was harvested and filtered through a 0.45- μ m filter.

To generate stable cell lines, HEK cells were then infected at ~50% confluency, followed by selection with 8 μ g/mL blasticidin in growth medium for at least 7 days before further analysis (Fig. 2c,d and Supplementary Figs. 8, 9a,b, 10c,e and 14a,b).

Biotin labeling with TurboID and miniTurbo in live mammalian cells. For labeling of transiently transfected cells, we initiated biotin labeling 18 to 36 h following transfection. From a 100 mM biotin stock in dimethyl sulfoxide (DMSO), we diluted biotin directly into serum-containing cell culture medium, to the desired final concentration. For BioID, we used a final concentration of 50 μ M biotin. For TurboID and miniTurbo, we typically used a final concentration of 500 μ M biotin (unless indicated otherwise). Labeling was stopped after the desired time period by transferring the cells to ice and washing five times with ice-cold PBS. Supplementary Figure 5 shows that cooling samples to 4 °C terminates the biotinylation reaction. For negative controls, we omitted exogenous biotin, or omitted the ligase.

Gels and Western blots. For gels and Western blots shown in Figures 1f and 2a,c and Supplementary Figures 1, 2, 4b, 5, 6, 8b–d, 9a and 10b,c, HEK 293T cells expressing the indicated constructs were plated, transfected, and labeled with biotin as described above, and subsequently detached from the flask by gently pipetting a stream of ice-cold PBS directly onto the cells. Pellets were collected by centrifuging the resulting cell suspension at 1,500 r.p.m. for 3 min. The supernatant was removed, and the pellet was lysed by resuspending in RIPA lysis buffer (50 mM Tris pH 8, 150 mM NaCl, 0.1% SDS, 0.5% sodium deoxycholate, 1% Triton X-100, 1 \times protease inhibitor cocktail (Sigma-Aldrich), and 1 mM PMSF) by gentle pipetting and incubating for 5 min at 4 °C. Lysates were clarified by centrifugation at 10,000 r.p.m. for 10 min at 4 °C. Protein concentration in clarified lysate was estimated with Pierce BCA Protein Assay Kit (ThermoFisher) prior to separation on a 9% SDS-PAGE gel. Silver-stained gels (Supplementary Figures 9a, 10b–c) were generated using Pierce Silver Stain Kit (ThermoFisher).

For the Western blot experiment in Figure 3a comparing ligase variants in the yeast cytosol, *S. cerevisiae* strain BY4741 cells were propagated at 30 °C in supplemented minimal medium (SMM; 6.7 g/L Difco nitrogen base without amino acids, 20 g/L dextrose, 0.54 g/L CSM –Ade –His –Leu –Lys –Trp –Ura (Sunrise Science Products), 20 mg/L adenine, 20 mg/L uracil, 20 mg/L histidine, 30 mg/L lysine) supplemented with leucine (100 mg/L). Yeast cells were transformed with pRS415 plasmids using the Frozen E-Z Yeast Transformation II kit (Zymoprep) according to manufacturer protocols. Transformed cells containing the *LEU2* gene were selected on SMM plates (SMM with 20 g/L agar) and propagated in SMM at 30 °C. Ligase expression was induced by inoculating saturated yeast culture into 10% D/G SMM (SMM medium with 90% of dextrose replaced with galactose) supplemented with 50 μ M biotin at a 1:100 dilution and incubating at 30 °C. After ~12 h, the saturated induced culture was diluted 1:30 in fresh induction media supplemented with 50 μ M biotin and allowed to grow for approximately 6 h more until reaching OD₆₀₀ ~1. Three milliliters of this culture was pelleted (normalized across samples so that the same approximate amount of cells are collected for each sample), and lysed on ice in 50 μ L 1.85 M NaOH + 300 mM β -mercaptoethanol for 10 min on ice. The protein in the lysate was then precipitated by adding 50 μ L 50% (w/v) TCA and incubating on ice for 15 min. The protein was pelleted at 12000g for 5 min, then dissolved in 120 μ L urea/SDS buffer (0.48 g/mL urea, 50 mg/mL SDS, 29.2 mg/mL EDTA, 15.4 mg/mL DTT, 1 mg/mL bromophenol blue, 12 mg/mL Tris base, 0.2 mL/mL 1M Tris pH 6.8). Proteins were boiled for 10 min prior to separation on a 9% SDS-PAGE gel.

For the Western blot experiment in Figure 3b comparing ligase variants in bacteria, BL21 *E. coli* bacteria expressing the indicated constructs (Supplementary Table 8) were induced overnight (18 h) at 37 °C in Lysogeny Broth (LB) supplemented with 100 μ g/mL ampicillin, 100 μ g/mL IPTG, and with or without 50 μ M biotin. Grown to approximately OD₆₀₀ = 0.6, 100 μ L of each culture was pelleted (normalized across samples so that the same approximate amount of cells are collected for each sample) and resuspended in 15 μ L

6 \times protein loading buffer (0.33 M Tris-HCl pH 8, 34% glycerol, 94 mg/mL SDS, 88 mg/mL DTT, 113 μ g/mL bromophenol blue). The protein was boiled for 5 min, diluted to 1 \times , and then separated on a 9% SDS-PAGE gel.

For all Western blots in Figures 1f, 2a,c and 3a,b and Supplementary Figures 1, 4b, 5, 6, 8b–d, 9a and 10b,c, proteins separated on SDS-PAGE gels were transferred to nitrocellulose membrane, and then stained by Ponceau S (5 min in 0.1% (w/v) Ponceau S in 5% acetic acid/water). The blots were then blocked in 5% (w/v) milk (LabScientific) in TBS-T (Tris-buffered saline, 0.1% Tween 20) for at least 30 min at room temperature, or as long as overnight at 4 °C. Blots were then stained with primary antibodies (Supplementary Table 9) in 3% BSA (w/v) in TBS-T for 1–16 h at 4 °C, washed four times with TBS-T for 5 min each, then stained with secondary antibodies or 0.3 μ g/mL streptavidin-HRP (Supplementary Table 9) in 3% BSA (w/v) in TBS-T for 1 at 4 °C. The blots were washed four times with TBS-T for 5 min each time before development with Clarity Western ECL Blotting Substrates (Bio-Rad) and imaging on a UVP BioSpectrum Imaging System, except for blots in Figures 1f, 2c and 3a,b, and Supplementary Figures 5a (miniTurbo) and 10b,c, which were imaged on a Bio-Rad Gel Doc 2000. Quantitation of Western blots was performed using ImageJ on raw images under non-saturating conditions.

Confocal fluorescence imaging of cultured cells. For fluorescence imaging experiments in Supplementary Figures 7, 8e, 9b, 10d,e and 14e,f, HEK 293T cells expressing the indicated constructs were plated, transfected, and labeled with biotin as described above, and subsequently fixed with 4% (v/v) paraformaldehyde in PBS at 4 °C for 45 min. Cells were then washed three times with PBS and permeabilized with cold methanol at -20 °C for 5 min. Cells were then washed three times with PBS, and then incubated with primary antibody (Supplementary Table 9) in PBS supplemented with 3% (w/v) BSA for 1 h at 4 °C. After washing three times with PBS, cells were then incubated with DAPI/secondary antibody, and neutravidin-Alexa Fluor647 (Supplementary Table 9) in PBS supplemented with 3% (w/v) BSA for 1 h at 4 °C. Cells were then washed three times with PBS and imaged by confocal fluorescence microscopy.

Confocal imaging was performed using a Zeiss AxioObserver.Z1 microscope, outfitted with a Yokogawa spinning disk confocal head, a Cascade II:512 camera, a Quad-band notch dichroic mirror (405/488/568/647), 405 (diode), 491 (DPSS), 561 (DPSS), and 640 (diode) nm lasers (all 50 mW). DAPI (405 laser excitation, 445/40 emission), Alexa Fluor568 (561 laser excitation, 617/73 emission), and Alexa Fluor647 (640 laser excitation, 700/75 emission), and differential interference contrast (DIC) images were acquired through a 63 \times oil-immersive objective; Acquisition times ranged from 50 to 100 ms. All images were collected and processed using SlideBook 6.0 software (Intelligent Imaging Innovations). The data in Supplementary Figures 7, 8e, 9b, 10d,e and 14e,f are representative of at least 10 fields of view.

Conjugation of AlexaFluor647 to neutravidin. A reaction mixture was assembled in a 1.5 mL Eppendorf tube with the following components (added in this order): 200 μ L of 5 mg/mL Neutravidin (Life Technologies) in PBS, 20 μ L of 1 M sodium bicarbonate in water, and 10 μ L of 10 mg/mL AlexaFluor647-NHS Ester (Life Technologies) in anhydrous DMSO. The tube was incubated at room temperature with rotation in the dark for 3 h. The neutravidin-AlexaFluor647 conjugate was purified from unreacted dye using a NAP-5 size-exclusion column (GE Healthcare Life Sciences) according to the manufacturer's instructions. The conjugate was typically eluted from the column in 500 μ L cold PBS. Absorbance values, determined using a Nanodrop 2000c UV-vis spectrophotometer (Thermo Scientific), were typically as follows: A280 = ~0.284 and A647 = ~1.625. The conjugate was stable at 4 °C in the dark for at least 4 months and was flash frozen and stored at 80 °C for longer term storage. For mammalian cell labeling experiments, the conjugate was diluted 1,000-fold in PBS containing 1% BSA.

Sample preparation for proteomics and for the Western blot experiment in Supplementary Figure 8. For each sample, HEK 293T cells were grown as a monolayer in 1:1 DMEM:MEM mixture (Cellgro) supplemented with 10% (w/v) fetal bovine serum (VWR), 50 μ g/mL penicillin, and 50 μ g/mL streptomycin in T150 flasks at 37 °C under 5% CO₂. Nuclear proteomic samples were generated by transfecting cells at approximately 60% confluency with

30 µg DNA using 150 µL Lipofectamine 2000 for 4 h. Mitochondrial matrix, ER membrane, and outer mitochondrial membrane samples were generated using HEK 293T cell lines that stably express the respective ligase. BioID samples were labeled using 50 µM biotin for 18 h; TurboID and miniTurbo samples were labeled using 500 µM biotin for 10 min. Labeling was stopped by placing cells on ice and washing five times with ice-cold PBS (**Supplementary Fig. 5**). Cells were detached from the flask by gently pipetting a stream of PBS directly onto the cells, then pellets were collected by centrifuging the resulting cell suspension at 1,500 r.p.m. for 3 min. The supernatant was removed, and the pellet was lysed in ~1.5 mL RIPA lysis buffer by gentle pipetting and incubating for 5 min at 4 °C. Lysates were clarified by centrifugation at 10,000 r.p.m. for 10 min at 4 °C.

To enrich biotinylated material from proteomic samples, 350 µL streptavidin-coated magnetic beads (Pierce) were washed twice with RIPA buffer, incubated with clarified lysates containing ~3 mg protein for each sample with rotation for 1 h at room temperature, then moved to 4 °C and incubated overnight with rotation. The beads were subsequently washed twice with 1 mL of RIPA lysis buffer, once with 1 mL of 1 M KCl, once with 1 mL of 0.1 M Na₂CO₃, once with 1 mL of 2 M urea in 10 mM Tris-HCl (pH 8.0), and twice with 1 mL RIPA lysis buffer. The beads were then resuspended in 1 mL fresh RIPA lysis buffer, transferred to a new Eppendorf tube, and shipped to Steve Carr's laboratory (Broad Institute) on ice for further processing and preparation for LC-MS/MS analysis.

For proteomic samples, 2.5% of the lysate was removed prior to enrichment used to estimate the protein concentration in clarified lysates using Pierce BCA Protein Assay Kit (ThermoFisher), as well as to verify ligase expression and confirm successful biotinylation by Western blotting as shown in **Supplementary Figures 9a and 10b,c**. After enrichment, 5% of beads were removed and biotinylated proteins were eluted by boiling the beads in 75 µL of 3× protein loading buffer supplemented with 20 mM DTT and 2 mM biotin. The eluted proteins were separated on an SDS-PAGE gel and stained using Pierce Silver Stain Kit to ensure that enrichment of biotinylated material was successful (**Supplementary Figures 9a and 10b,c**).

To enrich biotinylated material from samples prepared for **Supplementary Figure 8**, 240 µL streptavidin-coated magnetic beads (Pierce) were washed twice with RIPA buffer, incubated with clarified lysates containing approximately 3 mg protein for each sample with rotation for 1 h at room temperature. The beads were subsequently washed twice with 1 mL of RIPA lysis buffer, once with 1 mL of 1 M KCl, once with 1 mL of 0.1 M Na₂CO₃, once with 1 mL of 2 M urea in 10 mM Tris-HCl (pH 8.0), and twice with 1 mL RIPA lysis buffer. Biotinylated proteins were then eluted from the beads by boiling the beads in 300 µL of 3× protein loading buffer supplemented with 20 mM DTT and 2 mM biotin. For each sample, 25 µL of this eluate was then separated on SDS-PAGE gel alongside 35 µg protein from the corresponding clarified lysate prior to enrichment, and then transferred to nitrocellulose for Western blotting as described above with antibodies against the endogenous proteins indicated in **Supplementary Figure 8** (also see **Supplementary Table 9**).

On-bead trypsin digestion of biotinylated proteins. To prepare samples for mass spectrometry analysis, proteins bound to streptavidin beads (~300 µL of slurry) were washed twice with 200 µL of 50 mM Tris HCl buffer (pH 7.5) followed by two washes with 2 M urea/50 mM Tris (pH 7.5) buffer. The final volume of 2 M urea/50 mM Tris buffer (pH 7.5) was removed and beads were incubated with 80 µL of 2 M urea/50 mM Tris containing 1 mM DTT and 0.4 µg trypsin for 1 h at 25 °C with shaking. After 1 h, the supernatant was removed and transferred to a fresh tube. The streptavidin beads were washed twice with 60 µL of 2 M urea/50 mM Tris buffer (pH 7.5) and the washes were combined with the on-bead digest supernatant. The eluate was reduced with 4 mM DTT for 30 min at 25 °C with shaking. The samples were alkylated with 10 mM iodoacetamide for 45 min in the dark at 25 °C with shaking. An additional 0.5 µg of trypsin was added to the sample and the digestion was completed overnight at 25 °C with shaking. After overnight digestion, samples were acidified (to pH < 3) by adding formic acid (FA) such that the sample contained ~1% FA. Samples were desalted on C18 StageTips and evaporated to dryness in a vacuum concentrator, as previously described⁴⁶.

TMT labeling and fractionation of peptides. Desalted peptides were labeled with TMT (6-plex or 11-plex) reagents. Peptides were reconstituted in 100 µL of 50 mM HEPES. Each 0.8 mg vial of TMT reagent was reconstituted in 41 µL of anhydrous acetonitrile and added to the corresponding peptide sample for 1 h at room temperature. Labeling of samples with TMT reagents was completed with the design shown in **Figure 2d** and **Supplementary Figure 10a**. TMT labeling reactions were quenched with 8 µL of 5% hydroxylamine at room temperature for 15 min with shaking, evaporated to dryness in a vacuum concentrator, and desalted on C18 StageTips. For each TMT 6-plex cassette and the TMT 11-plex cassette, 50% of the sample was fractionated by basic pH reversed phase using StageTips while the other 50% of each sample was reserved for LC-MS analysis by a single-shot, long gradient. One StageTip was prepared per sample using 2 plugs of Styrene Divinylbenzene (SDB) (3M) material. The StageTips were conditioned two times with 50 µL of 100% methanol, followed by 50 µL of 50% MeCN/0.1% FA, and two times with 75 µL of 0.1% FA. Sample, resuspended in 100 µL of 0.1% FA, was loaded onto the stage tips and washed with 100 µL of 0.1% FA. Following this, sample was washed with 60 µL of 20mM NH₄HCO₂ /2% MeCN, this wash was saved and added to fraction 1. Next, sample was eluted from StageTip using the following concentrations of MeCN in 20 mM NH₄HCO₂: 10%, 15%, 20%, 25%, 30%, 40%, and 50%. For a total of 6 fractions, 10 and 40% (fractions 2 and 7) elutions were combined, as well as 15 and 50% elutions (fractions 3 and 8). The six fractions were dried by vacuum centrifugation.

Liquid chromatography and mass spectrometry. Desalted peptides were resuspended in 9 µL of 3% MeCN/0.1% FA and analyzed by online nanoflow liquid chromatography tandem mass spectrometry (LC-MS/MS) using an Orbitrap Fusion Lumos Tribrid MS (ThermoFisher Scientific) coupled online to a Proxeon Easy-nLC 1200 (ThermoFisher Scientific). Four microliters of each sample was loaded onto a microcapillary column (360 µm outer diameter × 75 µm inner diameter) containing an integrated electrospray emitter tip (10 µm), packed to approximately 24 cm with ReproSil-Pur C18-AQ 1.9 µm beads (Dr. Maisch GmbH) and heated to 50 °C. The HPLC solvent A was 3% MeCN, 0.1% FA, and the solvent B was 90% MeCN, 0.1% FA. The SDB fractions were measured using a 110 min MS method, which used the following gradient profile: (min:%B) 0:2; 1:6; 85:30; 94:60; 95:90; 100:90; 101:50; 110:50 (the last two steps at 500 nL/min flow rate). Non-fractionated samples were analyzed using a 260 min MS method with the following gradient profile: (min:%B) 0:2; 1:6; 235:30; 244:60; 245:90; 250:90; 251:50; 260:50 (the last two steps at 500 nL/min flow rate).

The Orbitrap Fusion Lumos Tribrid was operated in the data-dependent mode acquiring HCD MS/MS scans (resolution = 15,000 for TMT6-plex, or resolution = 50,000 for TMT11-plex) after each MS1 scan (resolution = 60,000) on the most abundant ions within a 2 s cycle time using an MS1 target of 3 × 10⁶ and an MS2 target of 5 × 10⁴. The maximum ion time utilized for MS/MS scans was 50 ms for TMT6-plex experiments and 105 ms for the TMT 11-plex experiment; the HCD normalized collision energy was set to 34 for TMT6 and 38 for TMT11; the dynamic exclusion time was set to 45 s, and the peptide match and isotope exclusion functions were enabled. Charge exclusion was enabled for charge states that were unassigned, 1 and >6.

Analysis of mass spectrometry data. Collected data were analyzed using Spectrum Mill software package v6.1pre-release (Agilent Technologies). Nearby MS scans with the similar precursor m/z were merged if they were within ± 60 s retention time and ±1.4 m/z tolerance. MS/MS spectra were excluded from searching if they failed the quality filter by not having a sequence tag length 0 or did not have a precursor MH⁺ in the range of 750 – 4000. All extracted spectra were searched against a UniProt⁴⁷ database containing human reference proteome sequences. Search parameters included: parent and fragment mass tolerance of 20 p.p.m., 30% minimum matched peak intensity, and 'calculate reversed database scores' enabled. The digestion enzyme search parameter used was Trypsin Allow P, which allows K-P and R-P cleavages. The missed cleavage allowance was set to 4. Fixed modifications were carbamidomethylation at cysteine. TMT labeling was required at lysine, but peptide N termini were allowed to be either labeled or unlabeled. Allowed variable modifications were protein N-terminal acetylation and oxidized methionine. Individual spectra were automatically assigned a confidence score using the

Spectrum Mill autovalidation module. Score at the peptide mode was based on target-decoy false discovery rate (FDR) of 1%. Protein polishing autovalidation was then applied using an auto thresholding strategy. Relative abundances of proteins were determined using TMT reporter ion intensity ratios from each MS/MS spectrum and the mean ratio is calculated from all MS/MS spectra contributing to a protein subgroup. Proteins identified by 2 or more distinct peptides were considered for the dataset.

Generation of proteomic lists for the ER membrane. Complete mass spectrometry data for the ER membrane (ERM) proteomic experiment are shown in **Supplementary Table 5**. To select cutoffs for proteins biotinylated by the indicated ligase over non-specific bead binders, we classified the detected proteins into three groups:

(1) ERM proteins (**Supplementary Table 2**; true positive list of 90 well-established ERM proteins³³).

(2) Soluble matrix proteins (**Supplementary Table 2**; false positive list of 173 soluble mitochondrial matrix proteins²).

(3) All other proteins

We then normalized the TMT ratios in order to account for differences in total protein quantity between samples within the TMT 11-plex experiment. To do this, the $\text{Log}_2(\text{TMT ratios})$ corresponding to ERM-ligase/untransfected ($\text{Log}_2(127\text{N}/126\text{C})$, $\text{Log}_2(128\text{N}/126\text{C})$, $\text{Log}_2(129\text{N}/126\text{C})$, ($\text{Log}_2(128\text{C}/126\text{C})$, $\text{Log}_2(130\text{N}/126\text{C})$, $\text{Log}_2(131\text{N}/126\text{C})$, $\text{Log}_2(131\text{C}/126\text{C})$) were normalized to the median for class (2) proteins, which was set to 0 (i.e. TMT ratios set to 1). To calculate optimal cut-offs, we then calculated the true positive rate (TPR) and false positive rate (FPR) we would obtain if we retained only proteins above that TMT ratio. We defined TPR as the fraction of class (1) proteins above the TMT ratio in question, and FPR as the fraction of class (2) above the TMT ratio in question. We selected TMT ratios that maximize the difference between TPR and FPR as our cutoffs (**Supplementary Fig. 9c**).

To select cutoffs for proteins biotinylated by the indicated ERM-ligase over proteins biotinylated by the corresponding cytosol-targeted ligase, we classified the detected proteins into three groups:

(1) ERM proteins (**Supplementary Table 2**; true positive list of 90 well-established ERM proteins³³).

(2) Non-secretory proteins (**Supplementary Table 2**; false positive list of 7421 human proteins that are not predicted to be secretory by Phobius⁴⁸ or are not annotated with the following Gene Ontology^{49,50} terms: GO:0005783, GO:0005789, GO:0007029, GO:0030867, GO:0048237, GO:0061163, GO:0016320, GO:0030868, GO:0006983, GO:0000139, GO:0051645, GO:0031985, GO:0005796, GO:0005795, GO:0005794, GO:0007030, GO:0090168, GO:0005886, GO:0007009, GO:1903561, GO:0070062, GO:0005576, GO:0031012, GO:0005615, GO:0005769, GO:0035646, GO:0005765, GO:0090341, GO:0090340, GO:0005635, GO:0007084, GO:0007077, GO:0006998, GO:0051081, GO:0005641, GO:0031965, GO:0005637, GO:0071765, GO:0048471, GO:1905719, GO:0031982, GO:0006906, GO:0048278, GO:0032587, GO:0016021, GO:0005887, GO:0005768, GO:0071816, GO:0031526, GO:0005913, GO:0072546, GO:1990440, GO:0030968, GO:1902236, GO:1990441, GO:0034976, GO:0005788, GO:0005790, GO:1902237, GO:0070059, GO:0005786, GO:0005793, GO:0044322, GO:0098554, GO:0005791, GO:1902010, GO:0043001, GO:0005802, GO:0006888, GO:0006890, GO:0005801, GO:0012510, GO:0006892, GO:0042147, GO:0034499, GO:0032588, GO:0006895, GO:0030140, GO:0051684, GO:0000042, GO:0032580, GO:0030173, GO:0006891, GO:0030198, GO:0031668, GO:0010715, GO:0035426, GO:1903053, GO:1903551, GO:0005578, GO:1903055, GO:0001560, GO:0022617, GO:0006887, GO:0012505).

(3) All other proteins

We then normalized the TMT ratios in order to account for differences in total protein quantity between samples within the TMT 11-plex experiment. To do this, the $\text{Log}_2(\text{TMT ratios})$ corresponding to ERM-ligase/ligase-NES ($\text{Log}_2(127\text{N}/127\text{C})$, $\text{Log}_2(128\text{N}/127\text{C})$, $\text{Log}_2(129\text{N}/129\text{C})$, ($\text{Log}_2(128\text{C}/129\text{C})$, $\text{Log}_2(130\text{N}/130\text{C})$, $\text{Log}_2(131\text{N}/130\text{C})$, $\text{Log}_2(131\text{C}/129\text{C})$) were normalized to the median for class (2) proteins, which was set to 0 (i.e. TMT ratios set to 1). To calculate optimal cut-offs, we then calculated the true positive rate (TPR) and false positive rate (FPR) we would obtain if we retained only proteins above that TMT ratio. We defined TPR as the

fraction of class (1) proteins above the TMT ratio in question, and FPR as the fraction of class (2) above the TMT ratio in question. We selected TMT ratios that maximize the difference between TPR and FPR as our cutoffs (**Supplementary Fig. 9c**).

After applying both cutoffs to each experimental replicate, we then intersected both filtered lists to produce the final proteomes (**Supplementary Table 5**). Overlap of proteins between proteomes obtained with BioID, TurboID 10 minute labeling, and TurboID 1 hour labeling are shown in **Supplementary Figure 9g**, **Supplementary Table 5**.

To assess the specificity of our proteomes (**Fig. 2e**), we report the percentage of proteins present in **Supplementary Table 2**, a list of 11,838 human proteins with secretory annotation according to Phobius⁴⁸, the Human Protein Atlas⁵¹ (protein localized to endoplasmic reticulum, Golgi apparatus, plasma membrane, vesicles, nuclear membrane, cell junctions; or predicted membrane proteins and predicted secreted proteins), the Plasma Proteome Database⁵², literature (reference cited in table), or are annotated with the following Gene Ontology^{49,50} terms: GO:0005783, GO:0005789, GO:0007029, GO:0030867, GO:0048237, GO:0061163, GO:0016320, GO:0030868, GO:0006983, GO:0000139, GO:0051645, GO:0031985, GO:0005796, GO:0005795, GO:0005794, GO:0007030, GO:0090168, GO:0005886, GO:0007009, GO:1903561, GO:0070062, GO:0005576, GO:0031012, GO:0005615, GO:0005769, GO:0035646, GO:0005765, GO:0090341, GO:0090340, GO:0005635, GO:0007084, GO:0007077, GO:0006998, GO:0051081, GO:0005641, GO:0031965, GO:0005637, GO:0071765, GO:0048471, GO:1905719, GO:0031982, GO:0006906, GO:0048278, GO:0032587, GO:0016021, GO:0005887, GO:0005768, GO:0071816, GO:0031526, GO:0005913, GO:0072546, GO:1990440, GO:0030968, GO:1902236, GO:1990441, GO:0034976, GO:0005788, GO:0005790, GO:1902237, GO:0070059, GO:0005786, GO:0005793, GO:0044322, GO:0098554, GO:0005791, GO:1902010, GO:0043001, GO:0005802, GO:0006888, GO:0006890, GO:0005801, GO:0012510, GO:0006892, GO:0042147, GO:0034499, GO:0032588, GO:0006895, GO:0030140, GO:0051684, GO:0000042, GO:0032580, GO:0030173, GO:0006891, GO:0030198, GO:0031668, GO:0010715, GO:0035426, GO:1903053, GO:1903551, GO:0005578, GO:1903055, GO:0001560, GO:0022617, GO:0006887, GO:0012505.

The specificity of the 'entire human proteome' reported in **Figure 2e** was calculated as the percentage of human proteins that are not present in category (2) non-secretory proteins, as defined above; i.e., the proteins that are present in the list of 11,838 human proteins with secretory annotation in **Supplementary Table 2**.

To calculate subsecretory specificity, we took a subset of proteins with the following Gene Ontology^{49,50} terms: GO:0005783 for endoplasmic reticulum, GO:0005794 for Golgi apparatus, and GO:0005886 for plasma membrane and classified them according to this priority: endoplasmic reticulum>Golgi apparatus>plasma membrane (**Supplementary Table 2**). We then took the subset of proteins in the ERM proteomes with these GO terms and plotted their percentages in **Figure 2f**. To calculate ER specificity, the subset of proteins with GOCC^{49,50} annotation for endoplasmic reticulum (GO:0005783) were subdivided into those with membrane annotation, soluble cytosolic annotation, or soluble luminal annotation according to GOCC^{49,50}, UniProt⁴⁷, TMHMM⁵³, or literature (**Supplementary Table 2**); these percentages are reported in **Figure 2g**.

To assess the recall/sensitivity of our ERM proteomes, we utilized a list of true positive ERM proteins (**Supplementary Fig. 9f**, **Supplementary Table 2**). In the scatter plots shown in **Supplementary Figure 9e**, true positive ERM proteins (**Supplementary Table 2**) are shown in green, cytosolic proteins (**Supplementary Table 2**; human proteins with Gene Ontology^{49,50} term GO:0005829 that lack annotated or predicted transmembrane domains according to UniProt⁴⁷ or TMHMM⁵³) are shown in red, and all other proteins are shown in black.

Generation of mitochondrial matrix and nuclear proteomic lists. Complete mass spectrometry data for both the nucleus and mitochondrial matrix are shown in **Supplementary Tables 6** and **7** respectively. Each of the two replicates for each proteomic experiment (mitochondrial matrix and nucleus) were analyzed separately. To select cutoffs for proteins biotinylated by the indicated ligase over non-specific bead binders, we classified the detected proteins into five groups:

(1) nuclear annotated proteins (**Supplementary Table 3**; true positive list of 6710 human proteins annotated with the following Gene Ontology^{49,50}

terms: GO:0016604, GO:0031965, GO:0016607, GO:0005730, GO:0001650, GO:0005654, GO:0005634).

(2) mitochondrial annotated proteins (**Supplementary Table 4**; true positive list of 1555 human proteins present in MitoCarta2.0 (ref. 54) or annotated with the following Gene Ontology^{49,50} term: GO:0005739, but excluding any proteins also present in category 2 (**Supplementary Table 4**).

(3) proteins with non-nuclear annotation (**Supplementary Table 3**; false positive list of 6815 human proteins annotated with the following Gene Ontology^{49,50} terms: GO:0015629, GO:0016235, GO:0030054, GO:0005813, GO:0045171, GO:0000932, GO:0005829, GO:0005783, GO:0005768, GO:0005929, GO:0005794, GO:0045111, GO:0005811, GO:0005764, GO:0005815, GO:0015630, GO:0030496, GO:0070938, GO:0005739, GO:0072686, GO:0005777, GO:0005886, GO:0043231; and are not annotated with the following Gene Ontology^{49,50} terms: GO:0016604, GO:0031965, GO:0016607, GO:0005730, GO:0001650, GO:0005654, GO:0005634, 'nucleus localization', 'nuclear envelope', 'nuclear matrix', 'nuclear chromatin', 'nuclear pore', 'nuclear inner membrane', 'nuclear chromosome', 'nuclear heterochromatin', 'nuclear euchromatin', 'nuclear inclusion body').

(4) proteins with non-mitochondrial annotation (**Supplementary Table 4**; previously curated false positive list of 2410 human proteins that are not annotated to be mitochondrial^{2,55}).

(5) All other proteins.

We then normalized the TMT ratios in order to account for differences in total protein quantity between samples within the TMT 6-plex experiments. To do this, the Log₂(TMT ratios) corresponding to ligase experiments/negative control (Log₂(126/127), Log₂(128/129), Log₂(130/131), Log₂(129/127) for replicate 1, and (Log₂(130/131), Log₂(129/126), Log₂(127/126) Log₂(128/126) for replicate 2) were normalized to the median for class (3) proteins for the nuclear dataset or class (4) proteins for the mitochondrial matrix data set, which was set to 0 (i.e. TMT ratios set to 1). To calculate optimal cut-offs, we then calculated the true positive rate (TPR) and false positive rate (FPR) we would obtain if we retained only proteins above that TMT ratio. We defined TPR as the fraction of class (1) proteins for the nuclear dataset or class (2) proteins for the mitochondrial matrix data set above the TMT ratio in question, and FPR as the fraction of class (3) proteins for the nuclear dataset or class (4) proteins above the TMT ratio in question. We selected TMT ratios that maximize the difference between TPR and FPR as our cutoffs (**Supplementary Fig. 10f,g**).

After applying cutoffs to each replicate, we then intersected both to produce the final proteomes (**Supplementary Table 6** for nuclear proteomes, **Supplementary Table 7** for mitochondrial matrix proteomes). Overlap of proteins between proteomes obtained with BioID, TurboID, and miniTurbo for both the nucleus and mitochondrial matrix are shown in **Supplementary Figure 10k**, **Supplementary Table 6** for nucleus, and **Supplementary Table 7** for mitochondrial matrix. To assess the specificity of our proteomes (**Figure 2h**), we calculated the percentage of proteins present in class (1) for the nuclear proteomes and class (2) for the mitochondrial matrix proteomes (**Supplementary Table 3** for nuclear specificity, **Supplementary Table 4** for mitochondrial specificity). To assess the recall/sensitivity of our proteomes, we determined the fraction of true positive proteins present in each proteome. 230 True positive nuclear proteins are shown in **Supplementary Table 3** and were assembled using Cell Atlas data (proteins detected by validated antibodies in nuclear bodies, nuclear membrane, nuclear speckles, nucleoli, fibrillary centers, nucleoplasm, or nucleus) and hyperLOPIT data⁵¹ (hyperLOPIT location annotated to nucleus, or nucleus-chromatin) and have been shown to be expressed in HEK cells⁵⁶. 173 True positive mitochondrial matrix proteins are obtained from previous work² and shown in **Supplementary Table 4**.

Generation of UAS-ligase transgenic Drosophila lines. V5-BioID, V5-TurboID, and V5-miniTurboID coding sequence was PCR amplified from CMV-plasmids using the same F and R primers:

V5-ligase_F: ccgcggccgccccctaccATGGGCAAGCCCATCCCC

V5-ligase_R gggtcgccgcgccccctctATTAGTCCAGGGTCAGGCG

DNA fragments were cloned into pEntr plasmids (Invitrogen) using Gibson assembly (NEB). pEntr_V5-ligase entry plasmids were recombined into pWalium10-roe⁵⁷ using Gateway LR Clonase II Enzyme (Invitrogen). pWalium10-roe contains 10× UAS enhancer elements for Gal4-controlled expression, attB sequence, and a white⁺ transgene. Transgenic flies were

generated using PhiC31 integration by injecting pWalium10-V5-ligase plasmids into flies carrying an attP docking site on chromosome III (attP2)⁵⁸. Final fly strains are referred to as UAS-V5-BioID, UAS-V5-TurboID, and UAS-V5-miniTurboID.

Drosophila culture and genetics. Experiments on flies were performed with wild type or transgenic strains of *Drosophila melanogaster*. The age and sex of animals involved in experiments are indicated in figure legends and methods below. The Harvard Medical School Standing Committee on Animals (through the Office of the Institutional Animal Care and Use Committee (IACUC)) deems flies as invertebrates with limited sentience and therefore not subject to formal review and approval by the committee.

Crosses were maintained on standard fly food at 25 °C. For temporal expression experiments using *tub-Gal4*, *tubGal80^{ts}*, animals were kept at 18 °C during all developmental stages until transferred to 29 °C to induce gene expression. Biotin food was prepared by microwaving standard fly food until liquid and adding 1 mM biotin dissolved in H₂O to a final concentration of 100 μM.

Unless otherwise noted, fly stocks were obtained from the Bloomington Drosophila Stock Center and are listed with the corresponding stock number: *ptc-Gal4* (2017), *Act5c-Gal4/CyO* (4414), *nub-Gal4* (25754), *w1118* (6326), *tub-Gal80^{ts}*; *tub-Gal4/TM6b* (Perrimon Lab), *UAS-Luciferase* (35788), *Desat-Gal4* (Oenocyte) (65405), *repo-Gal4* (Glia) (7415), *Mef2-Gal4* (Muscle) (27390), *Lpp-Gal4* (Fat body) (Perrimon Lab, see transgene in 67043 for information), *elav-Gal4* (Neurons) (8760), *Myo1a-Gal4* (Gut) (Perrimon Lab, see transgene in 67057 for information), *Hml-Gal4* (Hemocytes) (30140).

Western blotting of Drosophila adults. For experiments **Figure 3g** and **Supplementary Figure 12**, adult flies were aged 3 days after eclosion from pupal cases (13 days old after egg deposition). For each condition, five females and five males were lysed in RIPA buffer (Thermo Fisher, 89900) on ice using a blue pestle in a microcentrifuge tube. Samples were centrifuged at 14,000 xg for 20 min at 4 °C. Supernatant was retained and transferred to a new centrifuge tube. Protein concentration was calculated using a BCA kit (Pierce 23225) and RIPA buffer was added to samples to normalize to 4 μg/μL. Normalized protein samples were mixed with an equal volume of 4× SDS sample buffer and boiled for 5 min at 95 °C. 10 μg/sample was loaded onto a 4–20% Mini-PROTEAN TGX PAGE gel (Bio-Rad 4561095), transferred to Immobilon-FL PVDF membrane (Millipore IPFL00010), incubated in PBS + 0.1% Tween (PBST) for 15 min, and blocked overnight in 3% BSA in PBST (PBST-BSA) at 4 °C. To detect biotinylated proteins, blots were incubated with 0.3 μg/mL streptavidin-HRP (Thermo Fisher S911) in PBST-BSA for 1 hour at room temperature. Blots were washed extensively with PBST and exposed using Pico Chemiluminescent Substrate (Thermo Fisher 34577). To detect expressed V5-tagged ligases, blots were incubated with 1:10,000 mouse anti-V5 (Invitrogen R960-25) with PBST-BSA overnight at 4 °C, washed with PBST, incubated with 1:5000 anti-mouse Alexa 800 (Thermo Fisher A32730), washed with PBST, and imaged on an Aeries Fluorescent imager (LI-COR 9250).

Immunohistochemistry of Drosophila wing discs. For **Figure 3d**, wandering 3rd instar larvae were bisected and inverted to expose the imaginal discs. Inverted carcasses were fixed for 20 min in 4% paraformaldehyde in 1× PBS. Fixed carcasses with attached wing discs were permeabilized with PBS + 0.1% Triton-X100 (PBST) for 20 min and blocked with PBST + 5% normal goat serum (PBST-NGS) for 1 hour. Blocked carcasses were incubated overnight at 4 °C in PBST-NGS with 1:500 mouse anti-V5 (Invitrogen R960-25) and 1:500 streptavidin-555 (Invitrogen S32355). Carcasses were washed 3× with PBST and incubated for 1 hour at room temperature in PBST-NGS with 1:500 anti-mouse Alexa 647 (Thermo Fisher A-21236) and 1:1000 DAPI (stock 1mg/ml). Samples were washed with three times with PBST, once with PBS, and equilibrated in 70% Glycerol/1× PBS. Wing discs were dissected away from the carcass and mounted onto glass slides with Vectashield mounting media (Vector Labs H-1000) and glass coverslip. Mounted samples were imaged on a Zeiss 780 confocal microscope.

Quantitation of fluorescence signal intensity from Drosophila wing discs in Figure 3e. Average signal intensity of fluorescence of streptavidin-555 in wing discs was measured using raw images obtained under identical confocal settings and under non-saturating exposure settings. Using ImageJ software, the polygon tool was used to select a rectangular region of the *ptc-Gal4* expressing

domain in the wing pouch. The average signal intensity in this selected region was determined separately for the streptavidin-555 channel and the anti-V5 channel. The average signal intensity in control samples (very low background staining) was subtracted from signal intensity of experimental conditions (BioID, turboID, miniturnoID). For each wing disc, the signal intensity of streptavidin-555 was normalized to the signal intensity of anti-V5 (streptavidin-555/anti-V5). Fold change was determined by normalizing streptavidin-555/anti-V5 values from TurboID and miniturnoID to values from BioID. Measurements were taken from at least three wing discs for each condition.

Quantification of adult *Drosophila* wing size and survival after ligase expression during development in Supplementary Figure 13. *UAS-V5-ligase* transgenes were expressed during development by crossing with different Gal4-expressing lines and their effects on the adult assessed.

To determine if larval wing disc expression of ligases affects adult wing morphology, *nub-Gal4* was crossed with *UAS-V5-ligase* transgenes and the resulting progeny analyzed. *nub-Gal4* was crossed with wild-type flies (*w¹¹¹⁸*) as a negative control. Adult flies were aged 3 days after eclosion from pupal cases. Wings were removed from adults, placed in a drop of 50% Permout/50% Xylenes on a glass slide, and a coverslip added. Mounted wings were imaged using a light microscope with a 10× objective. Wing area was measured using the polygon selection tool in ImageJ. Wings quantified and imaged are from female flies.

To determine if developmental expression of ligases reduces survival to adulthood, we crossed *UAS-ligase* lines with different Gal4 lines that express in major tissue types (Muscle, Fat, Neurons, Glia, Gut, Oenocytes, Hemocytes) or ubiquitously (*Act5c-Gal4*). To quantify toxicity, we counted the number of surviving adult animals after undergoing ~10 days of development (from fertilized egg through pupal stages) expressing *UAS-ligase* under Gal4 control, and compared to the number of wild-type siblings. *UAS-Luciferase* was used as a negative control transgene, which is widely considered as non-toxic to cells.

As an example, the following crossing scheme was used for *Act5c-Gal4*:

P0 *Act5c-Gal4/CyO* × *UAS-V5-ligase* (homozygous)

Segregation of the *Act5c-Gal4* chromosome and *CyO* balancer chromosome results in two possible F1 progeny genotypes:

F1 (genotype 1) *Act5c-Gal4/UAS-V5-ligase*

F1 (genotype 2) *CyO/UAS-V5-ligase*

The *CyO* chromosome has a dominant *Cy* mutation that causes adult flies to have curly wings. Therefore genotype 1 flies have straight wings and express the ligase transgene, and genotype 2 have curly wings and do not express the transgene. The fraction of surviving flies expressing a given *UAS-transgene* is calculated as: # genotype 1/(# genotype 1 + # genotype 2)

For example, a survival fraction of 0.5 indicates that equal numbers of genotype 1 and genotype 2 were observed in the adult population, and that no reduction in survival from expressing a *UAS-transgene* during development occurred.

Similar crossing schemes were used for tissue-specific Gal4 lines. Gal4 lines that are normally maintained as a homozygous stock were first outcrossed to an appropriate balancer line to obtain Gal4/Balancer flies, which were then crossed with *UAS-Luciferase* or *UAS-TurboID*. Gal4 lines on chromosome II were used with a *CyO* balancer, and Gal4 lines on chromosome III were used with a *TM3, Sb* balancer.

Adult flies were aged >3 days after eclosion from pupal cases before being counted. Females and males of the same genotype were counted together.

For imaging whole adults, flies were frozen at -20 °C overnight and images of adult flies were obtained using a dissection microscope connected to a digital camera.

To determine if changes in the fraction of surviving flies were statistically significant, a two-sided Chi-square test was applied to the number of adult flies for genotype 1 and genotype 2, comparing *UAS-Luciferase* to a *UAS-ligase* transgene.

Mammalian cell viability assays. For each experiment presented in **Supplementary Figure 14**, five sterile, white, clear bottom 96-well plates were pre-coated with 100 μL 50 μg/mL human fibronectin in MEM for at least 20 min at 37 °C under 5% CO₂. For transiently transfected samples, HEK 293T cells were plated in 6-wells and transfected at ~90% confluency using 0.8 μL Lipofectamine2000 (Life Technologies) and 200 ng plasmid in serum-free

media (2.5 mL total volume) for 3-4 h, after which time Lipofectamine-containing media was replaced with fresh serum-containing media. After ~2 h, cells were trypsinized and seeded in triplicate into wells of each fibronectin-coated 96-well plate at 2000 cells/well in 50:50 serum-containing MEM: DMEM with or without 50 μM biotin. The stable cell lines were seeded into wells in the same manner. An additional triplicate of coated wells without cells served as background subtraction in each plate. One plate was immediately assayed after plating for cell viability by the CellTiter-Glo 2.0 Luminescent Viability assay (Promega). Subsequent plates were assayed at the indicated time points.

***C. elegans* strains and culture conditions.** Experiments on *Caenorhabditis elegans* were performed with wild type (N2) or transgenic strains expressing extrachromosomal arrays. The age and sex of animals involved in experiments are indicated in figure legends and methods below. The Stanford's Administrative Panel on Laboratory Animal Care (APLAC) deems *C. elegans* used in this study as invertebrates and not subject to formal review and approval by the committee.

Unless otherwise noted, *C. elegans* strains were cultured and maintained at 20 °C on *E. coli* OP50 bacteria as previously described⁵⁹. To deplete the animals of excess biotin, worms were grown for 2 generations on biotin auxotrophic *E. coli* (MG1655bioB:kan)⁶⁰ and washed twice with 1× M9 solution. Biotin auxotrophic *E. coli* MG1655bioB:kan was kindly donated by Dr. John E. Cronan, University of Illinois. Embryos dissected from one day-old adults of the following genotypes were compared for this study: JLF289 (wowEx66[ges1p::3×HA::BioID::unc-54, myo-2p::mCherry::unc-54]), JLF290 (wowEx67[ges1p::3×HA::BioID::unc-54, myo-2p::mCherry::unc-54]), JLF291 (wowEx68[ges1p::3×HA::TurboID::unc-54, myo-2p::mCherry::unc-54]), JLF292 (wowEx69[ges1p::3×HA::TurboID::unc-54, myo-2p::mCherry::unc-54]), JLF293 (wowEx70[ges1p::3×HA::miniTurbo::unc-54, myo-2p::mCherry::unc-54]), JLF294 (wowEx71[ges1p::3×HA::miniTurbo::unc-54, myo-2p::mCherry::unc-54]).

Transgenic ligase strain construction for *C. elegans*. *C. elegans* codon-optimized ligase genes BioID and TurboID (containing the 3 worm introns present in GFP) and miniTurbo (containing 2 worm introns present in GFP) were synthesized (IDT) and inserted into pJF241 to produce plasmids pAS28, pAS31, and pAS32, respectively. Transgenic worms were generated by injecting 50ng/μL ligase gene and 2.5ng/μL of the co-injection marker myo-2p::mCherry into day 1 N2 hermaphrodites.

Western blotting of *C. elegans* adults. Ligase expression and biotinylation (**Fig. 3i**, **Supplementary Fig. 15g**) were assessed by Western blotting one day-old adult worm lysates. For each condition, 50 N2 hermaphrodites (wild-type) or worms expressing a ligase transgene were transferred to Eppendorf tubes containing 1mL of M9 and washed once. Excess M9 was removed until ~50 μL of M9 remained and an additional 50 μL of 4× sample buffer was added. Worms were boiled at 95 °C for 10 min, vortexed 10 seconds, and centrifuged at 13,000×g for 5 min at 4 °C. Equal volume of lysate was loaded onto a 4-20% Mini-PROTEAN TGX PAGE gel (Bio-Rad), transferred to a nitrocellulose membrane (0.4 μm, Bio-Rad), and stained with Ponceau S solution. Blots were blocked in 5% milk PBST solution, probed with anti-HA (1:5000, rat monoclonal, Roche) and anti-tubulin (1:5000, rat monoclonal, Abcam) primary antibodies, and detected with secondary antibody (1:5000, goat anti-rat IRDye 680RD, Licor) and streptavidin-IRDye (1:5000, 800CW, Licor). Blots were imaged on LI-COR Odyssey CLx.

Immunohistochemistry and microscopy of *C. elegans*. To visualize ligases and biotinylation (**Fig. 3j**), embryos were isolated from one day-old adults, fixed, and stained as previously described⁶¹. Briefly, embryos were attached to poly-lysine coated microscope slides with Teflon spacers. Slides were frozen on dry ice and embryos were permeabilized by freeze-crack and fixed in 100% MeOH for 5 min at -20 °C. Embryos were washed in PBS then PBST, and subsequently incubated in anti-HA primary antibody (Abcam, 1:200) overnight at 4 °C to visualize ligase expression. Embryos were washed in PBST and then incubated in CY3-anti-mouse secondary antibody (Jackson ImmunoResearch Laboratories, 1:200) Streptavidin Alexa Fluor 488 (Invitrogen, 1:200), and

DAPI (Sigma, 1:10000). Embryos were mounted in Vectashield (Vector Laboratories) and stored at 4°C. Samples were imaged using 405 nm, 488 nm, and 561 nm lasers, a Yokogawa X1 confocal spinning disk head, and a 60× PLAN APO oil objective (NA=1.4) on a Nikon Ti-E inverted microscope (Nikon Instruments) equipped with a 1.5× magnifying lens. Images were captured using NIS Elements software (Nikon) and an Andor Ixon Ultra back thinned EM-CCD camera, at a sampling rate of 0.5µm. All samples were imaged with the same camera and laser settings, with the exception of embryos expressing miniTurbo. To avoid pixel saturation, a 25% reduction in camera exposure was used to capture the streptavidin-AF488 signal in miniTurbo expressing embryos. Thus, the miniTurbo images and quantifications in **Figure 3** for streptavidin-AF488 are an underrepresentation of the signal resulting from biotinylation. Images were processed and assembled in NIS Elements and Adobe InDesign. In **Figure 3j**, images shown are maximum intensity projections of two Z-slices with brightness adjusted for visual clarity.

Quantitation of fluorescence signal intensity in *C. elegans* intestine. Bean and comma stage embryos were chosen for analyses. For each embryo, one slice of the Z-stack was used for analysis. A custom Python script including the modules scikit-image, matplotlib, and NumPy combined with ImageJ was used to analyze *C. elegans* imaging data. A threshold for the HA:ligase signal was calculated by the Otsu method to create a mask to isolate the intestine region for each embryo. Background streptavidin-AF488 signal for each embryo was determined by drawing a square in the anterior portion of the embryo outside of the intestine and calculating the average pixel intensity within that square. The average background pixel intensity of streptavidin-AF488 was then subtracted from the average streptavidin-AF488 pixel intensity within the isolated intestine region, and the resulting corrected average was plotted for each embryo (**Fig. 3k**). To measure the ratio of streptavidin-AF488 to HA:ligase pixel intensities, each pixel value for streptavidin-AF488 within the isolated intestine region was corrected for background and then divided by its corresponding HA:ligase pixel value. Then the average of the ratio values for each embryo was plotted (**Supplementary Fig. 15**). Statistical significance was determined using the Mann-Whitney U test (**Fig. 3k**). Samples were blinded for statistical analysis.

Quantitation of *C. elegans* viability in Supplementary Fig. 16. *C. elegans* strains expressing ligase variants were maintained at 20 °C on either biotin+ (OP50) or biotin- (MG1655(bioB:kan)) *E. coli*. For BioID and TurboID in each bacteria condition, a one-day old adult worm expressing the ligase transgene from an extrachromosomal array and a sibling one-day old adult worm lacking the transgene (control) were placed on separate plates containing the appropriate bacteria. For each plate, the adult was removed after laying eggs for 4 hours and the remaining embryos on the plate were counted. Three days later the number of living worms were counted and viability was calculated by dividing the number of hatched worms by the number of eggs that were initially laid. Worms were kept on biotin+ or biotin- bacteria for two generations. Developmentally delayed worms were defined as worms that were larval stage or non-gravid at the time of counting.

Statistics. **Figure 3d,e**, wing disc imaging results are representative of at least 10 discs present on the microscope slide, and at least 3 of which were imaged. Sample sizes (n) in **e** from left column to right are 5, 6, 3. Error bars were calculated using s.e.m. This experiment was performed twice with similar results. **Supplementary Figure 13c**, sample sizes (n) from left column to right are 17, 14, 17, 15, 19, 18, 19, 18. Error bars were calculated using s.e.m. This experiment was performed twice with similar results. **Supplementary Figure 13d**, for each food type, a two-sided Chi-square test was used to determine if the difference in proportions (measure of effect) of UAS-ligase transgenes to UAS-Luciferase was statistically significant. Sample size values (n) from left column

to right: 512, 586, 466, 563, 286, 524, 513, 459. 95% confidence intervals (CI) for the difference in proportions of BioID, TurboID, and miniTurboID compared to Luciferase were -0.02945 to 0.09046, 0.2757 to 0.384, and -0.02958 to 0.09206 for normal food, and -0.04278 to 0.104, -0.05999 to 0.08728, and -0.07191 to 0.07838 for biotin food. p-values for all datapoints - Columns 1/2: 0.3113, Columns 1/3: <0.0001, Columns 1/4: 0.3027, Columns 5/6: 0.4109, Columns 5/7: 0.718, Columns 5/8: 0.9369. This experiment was performed twice with similar results. **Supplementary Figure 13f**, Data was analyzed as in **Supplementary Figure 13d**. Sample size values (n) from left column to right: 350, 367, 196, 339, 203, 284, 194, 287, 214, 232, 215, 305, 240, 346. 95% confidence intervals (CI) for each Gal4 line from left to right were -0.06874 to 0.0807, 0.04977 to 0.2228, -0.07546 to 0.1081, -0.03849 to 0.148, -0.07737 to 0.1115, 0.1398 to 0.3063, -0.07858 to 0.08951. p-values for all datapoints - Oenocytes: 0.8719, Glia: 0.0017, Muscle: 0.7295, Fat body: 0.2333, Neurons: 0.7143, Gut: <0.0001, Hemocytes: 0.8917. This experiment was performed twice with similar results.

Figure 3i, experiment was repeated 5 times with similar results, with the exception that miniTurbo expression was detectable in only 2 of those 5 replicates. Embryo imaging results shown in **Figure 3j** and **Supplementary Figure 15a** are representative images of complete quantitative data shown in **Figure 3k**. **Figure 3k** samples sizes (n) from left column to right column are 26, 18, 11, 16, 25, 8, 19, 23, 14, 14, 23, 9. Statistical significance was assessed via Mann-Whitney U test (two-sided). Error bars were calculated using s.e.m. **Supplementary Figure 15c-f**, statistical significance was assessed via Mann-Whitney U test (two-sided). Error bars were calculated using s.e.m. **Supplementary Figure 16a-c**, sample sizes (n) are indicated within an in column titled 'Replicates'. Statistical significance was assessed via Mann-Whitney U test (two-sided). Error bars were calculated using s.e.m.

For further detail on the experimental design, reagents, statistics, reproducibility, software, and data collection methods used in this study, please refer to the Life Sciences Reporting Summary.

Code availability. The Python script used for *C. elegans* imaging analysis is available from the corresponding author upon reasonable request.

Data availability. Source data for **Figure 2e** and **Supplementary Figures 8c-g** are provided in the paper in **Supplementary Table 5**. Source data for **Figure 2h** and **Supplementary Figure 9f-k** are provided in the paper in **Supplementary Tables 6 and 7**. The original mass spectra may be downloaded from MassIVE (<http://massive.ucsd.edu>) using the identifier: MSV000082304. The data is directly accessible via <ftp://massive.ucsd.edu/MSV000082304>. Any additional data that support the findings of this study are available from the corresponding author upon reasonable request.

38. Weaver, L.H., Kwon, K., Beckett, D. & Matthews, B.W. Corepressor-induced organization and assembly of the biotin repressor: a model for allosteric activation of a transcriptional regulator. *Proc. Natl. Acad. Sci. USA* **98**, 6045–6050 (2001).
39. Chao, G. *et al.* Isolating and engineering human antibodies using yeast surface display. *Nat. Protoc.* **1**, 755–768 (2006).
40. Jan, C.H., Williams, C.C. & Weissman, J.S. LOCAL TRANSLATION. response to comment on “Principles of ER cotranslational translocation revealed by proximity-specific ribosome profiling”. *Science* **348**, 1217 (2015).
41. Colby, D.W. *et al.* Engineering antibody affinity by yeast surface display. *Methods Enzymol.* **388**, 348–358 (2004).
42. Ausubel, F.M. *et al.* Current protocols in molecular biology. *Mol. Biol.* **1**, 13.2.1 (2003).
43. Wood, Z.A., Weaver, L.H., Brown, P.H., Beckett, D. & Matthews, B.W. Co-repressor induced order and biotin repressor dimerization: a case for divergent followed by convergent evolution. *J. Mol. Biol.* **357**, 509–523 (2006).
44. Xu, Y. & Beckett, D. Evidence for interdomain interaction in the *Escherichia coli* repressor of biotin biosynthesis from studies of an N-terminal domain deletion mutant. *Biochemistry* **35**, 1783–1792 (1996).
45. Eginton, C., Cressman, W.J., Bachas, S., Wade, H. & Beckett, D. Allosteric coupling via distant disorder-to-order transitions. *J. Mol. Biol.* **427**, 1695–1704 (2015).
46. Hung, V. *et al.* Spatially resolved proteomic mapping in living cells with the engineered peroxidase APEX2. *Nat. Protoc.* **11**, 456–475 (2016).

47. Apweiler, R. *et al.* UniProt: the universal protein knowledgebase. *Nucleic Acids Res.* **45**, D158–D169 (2017).
48. Käll, L., Krogh, A. & Sonnhammer, E.L.L. A combined transmembrane topology and signal peptide prediction method. *J. Mol. Biol.* **338**, 1027–1036 (2004).
49. Gene Ontology Consortium. Gene Ontology Consortium: going forward. *Nucleic Acids Res.* **43**, D1049–D1056 (2015).
50. Ashburner, M. *et al.*; The Gene Ontology Consortium. Gene ontology: tool for the unification of biology. *Nat. Genet.* **25**, 25–29 (2000).
51. Thul, P.J. *et al.* A subcellular map of the human proteome. *Science* **356**, eaal3321 (2017).
52. Muthusamy, B. *et al.* Plasma Proteome Database as a resource for proteomics research. *Proteomics* **5**, 3531–3536 (2005).
53. Krogh, A., Larsson, B., von Heijne, G. & Sonnhammer, E.L.L. Predicting transmembrane protein topology with a hidden Markov model: application to complete genomes. *J. Mol. Biol.* **305**, 567–580 (2001).
54. Calvo, S.E., Clauser, K.R. & Mootha, V.K. MitoCarta2.0: an updated inventory of mammalian mitochondrial proteins. *Nucleic Acids Res.* **44**, D1251–D1257 (2016).
55. Pagliarini, D.J. *et al.* A mitochondrial protein compendium elucidates complex I disease biology. *Cell* **134**, 112–123 (2008).
56. Sultan, M. *et al.* A global view of gene activity and alternative splicing by deep sequencing of the human transcriptome. *Science* **321**, 956–960 (2008).
57. Perkins, L.A. *et al.* The transgenic RNAi project at Harvard medical school: resources and validation. *Genetics* **201**, 843–852 (2015).
58. Markstein, M., Pitsouli, C., Villalta, C., Celnikier, S.E. & Perrimon, N. Exploiting position effects and the gypsy retrovirus insulator to engineer precisely expressed transgenes. *Nat. Genet.* **40**, 476–483 (2008).
59. Brenner, S. The genetics of *Caenorhabditis elegans*. *Genetics* **77**, 71–94 (1974).
60. Ortega-Cuellar, D. *et al.* Biotin starvation with adequate glucose provision causes paradoxical changes in fuel metabolism gene expression similar in rat (*Rattus norvegicus*), nematode (*Caenorhabditis elegans*) and yeast (*Saccharomyces cerevisiae*). *J. Nutrigenet. Nutrigenomics* **3**, 18–30 (2010).
61. Leung, B., Hermann, G.J. & Priess, J.R. Organogenesis of the *Caenorhabditis elegans* intestine. *Dev. Biol.* **216**, 114–134 (1999).

Reporting Summary

Nature Research wishes to improve the reproducibility of the work that we publish. This form provides structure for consistency and transparency in reporting. For further information on Nature Research policies, see [Authors & Referees](#) and the [Editorial Policy Checklist](#).

Statistical parameters

When statistical analyses are reported, confirm that the following items are present in the relevant location (e.g. figure legend, table legend, main text, or Methods section).

n/a Confirmed

- ☐ ☒ The exact sample size (*n*) for each experimental group/condition, given as a discrete number and unit of measurement
- ☐ ☒ An indication of whether measurements were taken from distinct samples or whether the same sample was measured repeatedly
- ☐ ☒ The statistical test(s) used AND whether they are one- or two-sided
Only common tests should be described solely by name; describe more complex techniques in the Methods section.
- ☒ ☐ A description of all covariates tested
- ☒ ☐ A description of any assumptions or corrections, such as tests of normality and adjustment for multiple comparisons
- ☐ ☒ A full description of the statistics including central tendency (e.g. means) or other basic estimates (e.g. regression coefficient) AND variation (e.g. standard deviation) or associated estimates of uncertainty (e.g. confidence intervals)
- ☐ ☒ For null hypothesis testing, the test statistic (e.g. *F*, *t*, *r*) with confidence intervals, effect sizes, degrees of freedom and *P* value noted
Give P values as exact values whenever suitable.
- ☒ ☐ For Bayesian analysis, information on the choice of priors and Markov chain Monte Carlo settings
- ☒ ☐ For hierarchical and complex designs, identification of the appropriate level for tests and full reporting of outcomes
- ☒ ☐ Estimates of effect sizes (e.g. Cohen's *d*, Pearson's *r*), indicating how they were calculated
- ☐ ☒ Clearly defined error bars
State explicitly what error bars represent (e.g. SD, SE, CI)

Our web collection on [statistics for biologists](#) may be useful.

Software and code

Policy information about [availability of computer code](#)

Data collection

ImageStudioLite was used to process Western blots imaged with Licor. UVP BioSpectrum Imaging System was used to acquire Western blots imaged with Clarity Western ECL Blotting Substrates (BioRad). Slidebook 6.0 was used to collect mammalian cell imaging data. BD CSM software was used to acquire the FACS data.

Data analysis

Slidebook 6.0 was used to analyze mammalian cell imaging data. ImageJ 1.50i was used to quantify Western blot data, Drosophila imaging data, and to measure Drosophila wing area. Prism 7.0 was used to analyze numerical data. BD FACSDIVA v8.0 was used to analyze the FACS data. A custom Python script including the modules scikit-image, matplotlib, and NumPy combined with ImageJ was used to analyze C. elegans imaging data. The script can be made available upon request. R statistical programming language and ggplot2 were used to analyze and plot numerical data for C. elegans data.

For manuscripts utilizing custom algorithms or software that are central to the research but not yet described in published literature, software must be made available to editors/reviewers upon request. We strongly encourage code deposition in a community repository (e.g. GitHub). See the Nature Research [guidelines for submitting code & software](#) for further information.

Data

Policy information about [availability of data](#)

All manuscripts must include a [data availability statement](#). This statement should provide the following information, where applicable:

- Accession codes, unique identifiers, or web links for publicly available datasets
- A list of figures that have associated raw data
- A description of any restrictions on data availability

Source data for Figure 2e and Supplementary Figures 8c-g are provided in the paper in Supplementary Table 25. Source data for Figure 2h and Supplementary Figures 9f-k are provided in the paper in Supplementary Tables 64 and 76. The original mass spectra may be downloaded from MassIVE (<http://massive.ucsd.edu>) using the identifier: MSV000082304. The data is directly accessible via <ftp://massive.ucsd.edu/MSV000082304>. Any additional data that support the findings of this study are available from the corresponding author upon reasonable request.

Field-specific reporting

Please select the best fit for your research. If you are not sure, read the appropriate sections before making your selection.

☒ Life sciences ☐ Behavioural & social sciences ☐ Ecological, evolutionary & environmental sciences

For a reference copy of the document with all sections, see nature.com/authors/policies/ReportingSummary-flat.pdf

Life sciences study design

All studies must disclose on these points even when the disclosure is negative.

Sample size	All mammalian cell imaging results presented were representative of at least 10 independent fields of view. Sample size of mammalian cell image fields of view was chosen in consistency with many other publications (e.g. PMID: 28650461). Drosophila fly wing disc imaging results are representative of at least 10 discs present on the microscope slide, at least 3 of which were imaged. Full information on sample size in figure legend and methods. Sample size of imaged wing discs was chosen as the maximum number of samples processed at the same time without sacrificing consistency of tissue fixation, antibody staining, and slide mounting. The number of adult flies counted for survival assays was performed to maximize accuracy, at least 286 adult flies/sample were counted. Full information on sample size in figure legend and methods. Sample size of counted surviving adults was chosen as the maximum possible number of progeny flies collected from a single cross to control for variables such as food quality. The number of flies counted is consistent with published protocols on quantifying survival in Drosophila (PMID: 24751824). Measurements of wing size from adult flies were performed on at least 14 wings. Full information on sample size in figure legend and methods. Images and quantification of Drosophila flies and tissues were representative of results. Sample size is indicated in Figure 3 and Supplementary Figure 12 legends. Sample size of wings were chosen as the maximum number of wings processed at the same time. The number of wings quantified is consistent with many other publications (e.g. PMID: 25107277). For all C. elegans experiments, full information on sample size and replicates are within figures, figure legends, and/or methods. Images and quantifications shown in Figure 3 and Supplementary figures and qualifications are representative of results. For consistency, two specific stages of worm embryonic development were chosen for IF staining. Sample size of embryos imaged were chosen as the maximum number of samples processed at the same time.
Data exclusions	For consistency, a specific stage of worm development was chosen (embryos). Embryos within that stage were chosen for quantitative analysis.
Replication	The number of times an experimental finding was reproduced is indicated in the associated figure legend for each experiment shown. For Figure 3i, the experiment was performed five times (n = 5). In biotin+ conditions, BioID biotinylation activity was undetectable and TurboID gave robust biotinylation signal in all replicates (n = 5/5). Despite high activity detected by immunofluorescence in embryos, we only detected some low level of biotinylation by miniTurbo in adults (n = 2/5), likely due to its low expression levels. For all other experiments, attempts at replication were successful.
Randomization	No randomization methods were used because this was not applicable for our experiments. Randomization of adult flies or larvae was not used because freely-moving animals are too small to be assigned numbers for subsequent random selection. Fly wing discs and adult wings were selected for imaging randomly, and adult flies were selected for lysis and western blotting randomly. Randomization does not apply to counting survival of adult flies since all flies are counted. Worm embryos were selected for imaging randomly, and adult worms were selected randomly for lysis and subsequent Western blotting. Randomization does not apply to counting survival and developmental delay of worms since all worms in these experiments were counted.
Blinding	Investigator was blinded to group allocation during statistical analyses for C. elegans experiments.

Reporting for specific materials, systems and methods

Materials & experimental systems

n/a	Involved in the study
<input checked="" type="checkbox"/>	<input type="checkbox"/> Unique biological materials
<input type="checkbox"/>	<input checked="" type="checkbox"/> Antibodies
<input type="checkbox"/>	<input checked="" type="checkbox"/> Eukaryotic cell lines
<input checked="" type="checkbox"/>	<input type="checkbox"/> Palaeontology
<input type="checkbox"/>	<input checked="" type="checkbox"/> Animals and other organisms
<input checked="" type="checkbox"/>	<input type="checkbox"/> Human research participants

Methods

n/a	Involved in the study
<input checked="" type="checkbox"/>	<input type="checkbox"/> ChIP-seq
<input type="checkbox"/>	<input checked="" type="checkbox"/> Flow cytometry
<input checked="" type="checkbox"/>	<input type="checkbox"/> MRI-based neuroimaging

Antibodies

Antibodies used

antibody, vendor, catalog number/lot number: mouse anti-myc, Calbiochem, OP10/D00158557; goat anti-mouse-HRP, BioRad, 170-6516; chicken anti-myc, Invitrogen, A-21281/1819879; goat anti-chicken-AlexaFluor647, Invitrogen, A21449/1081817; rabbit anti-biotin, ImmuneChem, ICP0611; goat anti-rabbit-R-phycoerythrin, Life Technologies, P2771MP; mouse anti-V5, Invitrogen, 46-0705/1847319/1865511; mouse anti-calreticulin, Calbiochem, 208912/D00154827; mouse anti-BCAP31, Proteintech, 11200-1-AP/00018537; rabbit anti-Tom70, Proteintech, 14528-1-AP/00005668; mouse anti-Tom20, Santa Cruz Biotechnology, sc-17764/B2117; mouse anti-HXK I, Santa Cruz Biotechnology, sc-46695/F1611; rabbit anti-NDUFS6, Abcam, ab195808; rabbit anti-calnexin, Santa Cruz Biotechnology, sc-11397/11914; rabbit anti-Tom20, Santa Cruz Biotechnology, sc-11415/12711; goat anti-rabbit-AlexaFluor568, Invitrogen, A-11011/1704462; mouse anti-His6, Calbiochem, OB05; goat anti-mouse-AlexaFluor647, Invitrogen, A21236; goat anti-mouse-AlexaFluor800, Invitrogen, A32730/RJ243418; mouse anti-HA, Abcam, ab130275/GR250145-5; goat anti-mouse-CY3, Jackson ImmunoResearch Laboratories, 115-165-166/117091; rat anti-alpha tubulin, Abcam, ab6161; rat anti-HA, Roche, 11867423001; goat anti-rat IRDye 680RD, LI-COR, 92568076/C61115-06.

Validation

mouse anti-myc (Calbiochem, OP10): Epitope Tagging - Munro, S., et al. 1986. Cell 46, 291. Immunoblotting - Evan, G.I., et al. 1985. Mol. Cell. Biol. 5, 3610; chicken anti-myc (Invitrogen, A-21281): several published flow cytometry applications cited on website - <https://www.thermofisher.com/antibody/product/Myc-Tag-Antibody-Polyclonal/A-21281>; rabbit anti-biotin (ImmuneChem, ICP0611): Udeshi et al in Nature Methods Vol.14 pages: 1167-1170 (2017); mouse anti-V5 (Invitrogen, 46-0705): several published immunofluorescence and Western blotting applications cited on website - <https://www.thermofisher.com/antibody/product/V5-Tag-Antibody-Monoclonal/R960-25>; mouse anti-calreticulin (Calbiochem, 208912): Nauseef, W.M., et al. 1995. J. Biol. Chem. 270, 4741. Jethmalani, S.M., et al. 1994. J. Biol. Chem. 269, 23603. Smith, M.J., and Koch, G.L.E. 1989. EMBO J. 8, 3581; mouse anti-BCAP31 (Proteintech, 11200-1-AP): validation shown on website - <https://www.ptglab.com/products/BCAP31-Antibody-11200-1-AP.htm#validation>; rabbit anti-Tom70 (Proteintech, 14528-1-AP): validation shown on website - <https://www.ptglab.com/products/TOM70-Antibody-14528-1-AP.htm#validation>; mouse anti-Tom20 (Santa Cruz Biotechnology, sc-17764): several published applications cited on website - <https://www.scbt.com/scbt/product/tom20-antibody-f-10>; mouse anti-HXK I (Santa Cruz Biotechnology, sc-46695): several published applications cited on website - <https://www.scbt.com/scbt/product/hxk-i-antibody-g-1?requestFrom=search>; rabbit anti-NDUFS6 (Abcam, ab195808): validation shown on website - <http://www.abcam.com/ndufs6-antibody-epr15957-37-ab195808.html>; rabbit anti-calnexin (Santa Cruz Biotechnology, sc-11397): several published applications cited on website - <https://www.scbt.com/scbt/product/calnexin-antibody-h-70?requestFrom=search>; rabbit anti-Tom20 (Santa Cruz Biotechnology, sc-11415): several published applications cited on website - <https://www.scbt.com/scbt/product/tom20-antibody-fl-145>; mouse anti-His6 (Calbiochem, OB05): Zentgraf, H., et al. 1995. Nucl. Acids. Res. 23, 3347. Gu, J., et al. 1994. BioTechniques 17, 257. Sporeno, E., et al. 1994. J. Biol. Chem., 10991. Sisk, W.P., et al. 1994. J. Virol. 68, 766. Lu, T., et al. 1993. Anal. Biochem. 213, 318. Garner, J., et al. 1992. Cell 69, 833. Hochuli, E., et al. 1987. J. Chromatogr. 411, 177; mouse anti-HA (Abcam, ab130275): several published applications cited on website - <http://www.abcam.com/ha-tag-antibody-16b12-ab130275-references.html>; rat anti-alpha tubulin (Abcam, ab6161): several published applications cited on website - <http://www.abcam.com/tubulin-antibody-yol134-microtubule-marker-ab6161-references.html>; rat anti-HA (Roche, 11867423001): several published applications cited on website - https://www.sigmaaldrich.com/catalog/product/roche/roahaha?lang=en®ion=US&gclid=CjwKCAjwma3ZBRBwEiwA-CsbILDleASZObnaR5a0aQ7M7VoYt3ZrFhFWajwsOc-IazvFLIHOW_VzRoCPycQAvD_BwE.

Eukaryotic cell lines

Policy information about [cell lines](#)

Cell line source(s)

The source of the HEK 293T cell line was ATCC.

Authentication

The cell line (HEK293T) was not authenticated.

Mycoplasma contamination

The cells were not tested for mycoplasma contamination.

Commonly misidentified lines
(See [ICLAC](#) register)

None. The only cell line used in this paper is HEK293T, which is not listed in the ICLAC database.

Animals and other organisms

Policy information about [studies involving animals](#); [ARRIVE guidelines](#) recommended for reporting animal research

Laboratory animals

Experiments on flies were performed with wild type or transgenic strains of *Drosophila melanogaster*. The age and sex of animals

Laboratory animals

involved in experiments are indicated in figure legends and methods below. Unless otherwise noted, fly stocks were obtained from the Bloomington Drosophila Stock Center and are listed with the corresponding stock number: ptc-Gal4 (2017), Act5c-Gal4/CyO (4414), nub-Gal4 (25754), w1118 (6326), tub-Gal80ts; tub-Gal4/TM6b (Perrimon Lab), UAS-Luciferase (35788), Desat-Gal4 (Oenocyte) (65405), repo-Gal4 (Glia) (7415), Mef2-Gal4 (Muscle) (27390), Lpp-Gal4 (Fat body) (Perrimon Lab, see transgene in 67043 for information), elav-Gal4 (Neurons) (8760), Myo1a-Gal4 (Gut) (Perrimon Lab, see transgene in 67057 for information), Hml-Gal4 (Hemocytes) (30140). All Details on the flies used are provided in the methods section and figure legends. *Caenorhabditis elegans* experiments involved embryos or, hermaphrodite adultss. The age of animals involved in experiments are indicated in figure legends or methods. N2 wild-type strain was obtained from the *Caenorhabditis* Genetics Center (CGC).

Wild animals

None.

Field-collected samples

None.

Flow Cytometry

Plots

Confirm that:

- ☒ The axis labels state the marker and fluorochrome used (e.g. CD4-FITC).
- ☒ The axis scales are clearly visible. Include numbers along axes only for bottom left plot of group (a 'group' is an analysis of identical markers).
- ☒ All plots are contour plots with outliers or pseudocolor plots.
- ☒ A numerical value for number of cells or percentage (with statistics) is provided.

Methodology

Sample preparation

All FACS experiments in this study used yeast. Sample preparation is described in detail in the following methods sections: Yeast cell culture, Generation of BirA libraries for yeast display, Yeast display selections, Directed evolution of TurboID and miniTurbo.

Instrument

Yeast display FACS sorting was performed on BD FACS Aria II cell sorter, and all FACS analysis was performed on BD Accuri flow cytometer.

Software

BD FACSDIVA software was used to perform FACS sorts and analyze all data. FACS analysis data (performed on BD Accuri flow cytometer) was collected using BD CSampler software.

Cell population abundance

Percentages of pre- and post-sort cell populations analyzed and sorted are described in detail in the following methods sections: Yeast display selections, Directed evolution of TurboID and miniTurbo.

Gating strategy

Descriptions of the gating strategies used are included in the methods sections "Yeast display selections" and "Directed evolution of TurboID and miniTurbo" and are exemplified in Supplementary Figure 2j.

- ☒ Tick this box to confirm that a figure exemplifying the gating strategy is provided in the Supplementary Information.